

Postprint

Earth-Science Reviews ISSN 1872-6828, Vol. 199, article 102978, 2019

1 **Measuring techniques for concentration and stable isotopologues of CO₂ in a**
2 **terrestrial ecosystem: A review**

3

4 *Grega E. Voglar¹*, Saša Zavadlav¹, Tom Levanič¹, Mitja Ferlan¹*

5

6 *¹Slovenian Forestry Institute, Večna pot 2, SI-1000 Ljubljana, Slovenia*

7

8 **Corresponding author, e-mail: grega.voglar@gozdis.si, Tel: +386-01-200-7842*

9 **1. Introduction**

10 With increasing emphasis on the carbon dioxide (CO₂) effect on climate dynamics
11 (Pachauri et. al, 2014), monitoring the carbon exchange between the atmosphere and
12 terrestrial ecosystems and carbon cycling in ecosystems is of essential importance for
13 understanding climate change (Vaughn et al., 2010; Schimel et al., 2015). The stable
14 isotopes of carbon ($\delta^{13}\text{C}$) track changes in photosynthesis, respiration, organic matter
15 decomposition and anthropogenic fuel emission inputs (e.g., McDowell et al., 2008),
16 while the oxygen isotopes of water ($\delta^{16}\text{O}$ and $\delta^{18}\text{O}$) contain information on the linkages
17 between the carbon and water cycles (Dawson and Simonin, 2011). Analysis of both the
18 concentrations and isotopic composition of CO₂ is a useful tool for tracing,
19 characterizing and quantifying the CO₂ cycle on temporal and spatial scales.
20 Concentration measurements of CO, NO_x, CO₂, etc. became widespread in the mid-
21 1960s, when the first semiconductor diode lasers were developed to trace its cycle in
22 different applications. Much of this instrumentation is based on near- and mid-infrared
23 absorption spectroscopy, spanning wavelengths from 1 to >10 μm (McDonagh et al.,
24 2008). The traditional spectroscopic technique has been non-dispersive infrared
25 (NDIR), by which the transmission has been measured at two wavelength regions, one
26 at absorbing and the other at non-absorbing wavelengths (Linnerud et al., 1998). Fourier
27 transform infrared (FTIR) spectroscopy is an alternative to NDIR-based analysers and
28 has advantages because of a high-throughput and being well-suited to multicomponent
29 analysis of gases and other chemical elements/compounds.

30 Through continuous progress, the stable isotope techniques have become widespread in
31 environmental sciences (Hoefs, 2009; Michener & Lajhta, 2008 and West et al., 2011)
32 and, over recent decades, our understanding of environmental changes and, in

33 particular, of carbon fluxes and carbon-water relations, has considerably improved
34 owing to the development (and employment) of precise and accurate isotope ratio mass
35 spectrometry (IRMS) and laser-absorption spectroscopy (LAS) measurement techniques
36 (e.g., Crosson et al., 2002; Erdelyi et al., 2002; Griffis, 2013; Kerstel et al., 1999;
37 Mortazavi and Chanton, 2002; Muccio and Jackson, 2009; Saleska et al., 2006; Schauer
38 et al., 2005; Schnyder et al., 2004; Theis et al., 2004; Wada et al., 2016; West et al.,
39 2011; Wen et al., 2013; Wehr et al., 2013, Wehr et al., 2016 and Wehr et al., 2017).
40 Stable isotope abundance measurements require highly precise mass spectrometers
41 (defined generally as a standard deviation in the range of 4 to 6 significant figures, i.e.,
42 parts per thousand) (Brenna, 1997; Brenna et al., 1997), allowing the introduction of
43 simple analytes. The samples for off-line IRMS must first be converted into a gaseous
44 form (e.g., CO₂, N₂, SO₂, CO etc.) and later introduced for analyses. On-line sample
45 inlet systems were introduced with the development of the continuous-flow IRMS
46 measurement technique in the 1980s, which allowed a faster and higher throughput of
47 samples. In the early 1990s, the first LAS techniques were employed for stable isotope
48 ratio measurements in air samples and are nowadays widely used in the analysis of trace
49 gases, including CO₂ isotopologues (Werle, 1998).

50 While LAS is readily field-deployable and widely implemented, the IRMS techniques
51 are more oriented to laboratory usage (McAlexander et al., 2011). The choice of which
52 technique to use highly depends on the research questions, remoteness of the study area
53 and financial capacities. However, regardless of the study aims, the type of analytical
54 instrument chosen should meet the required sensitivity and must be insensitive to
55 vibrations and mechanical instabilities when used for measurements in the field. In this
56 paper, we outline the strengths and weaknesses of both IRMS and LAS analytical

57 techniques for concentration and stable isotope ratio measurements of CO₂, highlighting
58 some examples of ecological research campaigns.

59 **2. Methodology**

60 This review focused on papers that used IRMS and LAS analytical techniques for
61 concentration and stable isotopologues of CO₂ measurement. To refine the pool of
62 searched literature that met our criteria, Scopus and Web of Science, as two of the
63 world's largest citation databases, were used. At each query, terms and keywords such
64 as 'CO₂ isotopologues', 'laser-absorption spectroscopy', 'isotope ratio mass
65 spectrometry', 'isotope analyser', 'CO₂', 'trace gas', 'stable isotopes', 'decision tree'
66 and 'terrestrial ecosystem' were used individually to produce an extensive list of
67 articles. Using Scopus and Web of Science, the body of literature was searched based
68 on a fixed set of inclusion criteria: 1) The search was set from the date of the first
69 relevant article until until early 2019, 2) The predefined keywords should exist as a
70 whole in at least one of the fields: title, keywords or abstract, 3) The paper should be
71 published in a scientific peer-reviewed journal and 4) The paper should be written in the
72 English language. The outcome of this review is presented in Results and Discussion
73 and Conclusions and Outlook sections.

74 **3. Results and Discussion**

75 **3.1 CO₂ sample collection and treatment for stable isotope ratio measurements**

76 Long-term measurements of CO₂ concentration and stable carbon and oxygen isotope
77 ratio measurements based on hourly or minute scale (LAS) or periodic sampling
78 (IRMS) are essential for understanding CO₂ dynamics in the environment.

79 Isotopologues of carbon dioxide (e.g. $^{12}\text{C}^{16}\text{O}_2$, $^{13}\text{C}^{16}\text{O}_2$, $^{12}\text{C}^{17}\text{O}_2$, $^{12}\text{C}^{18}\text{O}_2$, $^{13}\text{C}^{17}\text{O}_2$ and
80 $^{13}\text{C}^{18}\text{O}_2$) are key tools for investigating CO_2 gas exchanges and have been valuable in
81 assessing the proportion of ecosystem respiration of CO_2 (Bowling et al, 2003) and
82 investigating the dynamics of the atmospheric surface layer within forest canopies
83 (Bowling et al. 1999). Stable isotopes of CO_2 have recently been used on a global scale
84 to study the magnitude and nature of carbon exchange between terrestrial ecosystems
85 and the atmosphere (Bowling et al., 2003; Ogée et al. 2003 and van Geldern et al.
86 2014), while Guillon et al. (2012) identified carbon sources by monitoring stable
87 isotope changes in CO_2 degassing from an underground tunnel. Both IRMS and LAS
88 techniques have great ability for the detection and monitoring of constituents in gas
89 phases and enabling a complete understanding of terrestrial ecosystem dynamics in
90 response to varying environmental conditions. The main limitation when using
91 laboratory (off-line) IRMS facilities is the low frequency of sampling and relatively
92 high analysis costs. The air or soil CO_2 samples are collected manually by employing
93 syringes and vials for storage, although several automated devices for collection of air
94 samples have been developed (Ribas-Carbo et al., 2002; Schauer et al., 2005; Schnyder
95 et al., 2004 and Theis et al., 2004) and tested for their performance and precision (see
96 decision tree diagram, section 3.5). Moreover, even portable gas sampling units
97 connected to IRMS have been employed (Schnyder et al., 2004).

98 Commercially available gas sample preparation systems (e.g., Isoprime TraceGas
99 preconcentrator, Thermo-Finnigan Precon and GasBench, Europa Anca TG-II) involve
100 processing volumes of air of more than 100 mL (Zeeman et al., 2008) through a set of
101 chemical traps that remove water and purify the analyte CO_2 , which is later
102 concentrated cryogenically with liquid N_2 . For the estimation of the carbon net

103 ecosystem exchange, sources or respiration sources, CO₂ concentrations must also be
104 measured (Keeling, 1958) and although IRMS instruments are not primarily devoted to
105 gas concentration measurements, some studies have attempted to do so. Joos et al.
106 (2008) determined CO₂ concentrations based on the peak areas of mass-to-charge ratios
107 (m/z) 44, 45 and 46, with a precision of 3.5 to 13.1 ppm within a concentration range
108 from 300 to 1000 ppm. Other reports coupling IRMS with an infra-red gas analyser
109 (IRGA) (Ferretti et al., 2000 and Schnyder et al., 2004) or NDIR (Schauer et al., 2005)
110 gave measurement precisions below 1 ppm (see decision tree diagram, section 3.5).

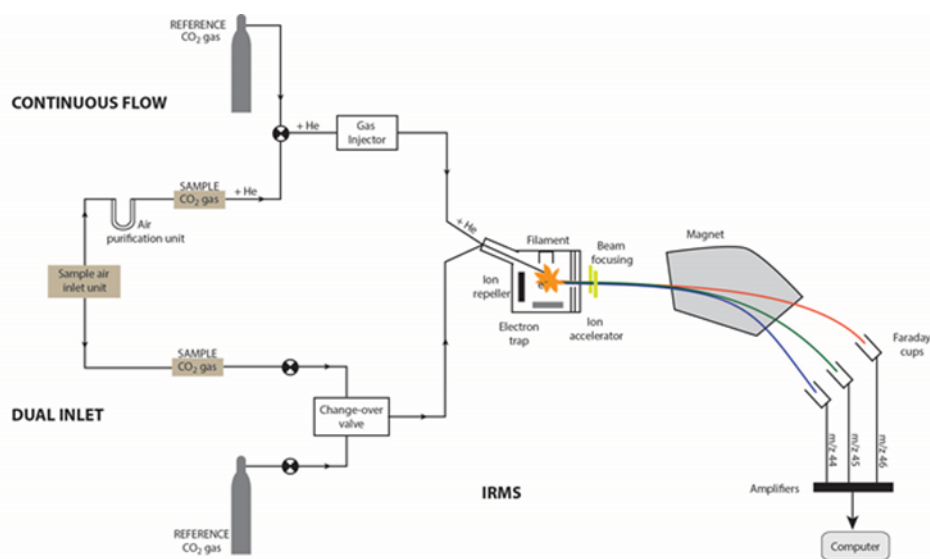
111 ***3.2 Measuring stable isotope ratios of CO₂ with IRMS***

112 In 1919, Francis W. Aston built an early double-focusing mass spectrometer in
113 Cambridge (UK) (Fry, 2006) but the first accurate measurements of isotope abundances
114 in gases were made by Alfred O. C. Nier (Nier, 1940) by placing a multi-collector into a
115 mass spectrometer. Stable isotope ratios of substances are most commonly measured
116 with a stable isotope ratio mass spectrometer (IRMS) that, in principal, separates
117 charged atoms or molecules based on their m/z . The ratios of stable carbon and oxygen
118 isotopes are always measured relative to a reference with known isotopic composition
119 to eliminate any bias or systematic error in the measurements (Muccio and Jackson,
120 2009). There are five main components of an IRMS instrument: a sample inlet system,
121 an ionization chamber, a magnetic sector for ion separation, a Faraday-collector for ion
122 detection, and a computer-controlled data acquisition system (Brand, 2004 and
123 Sulzman, 2007) (Fig. 1).

124 Once the sample (or reference) gas leaves the inlet system, it enters the ionization
125 chamber, where is bombarded with electrons produced from heated wire of tungsten,
126 rhenium or thoriated iridium (Brand, 2004). The electrons impact gas molecules,

127 forming positively charged ions that are gathered into an ion beam, which is further
 128 accelerated by an electrical field through a set of extraction and focusing plates towards
 129 the flight tube. The ion beam then enters the magnetic sector of the mass spectrometer,
 130 where it is bent by a strong magnetic field based on the mass of the ions, with the lighter
 131 isotope beams bending more than the heavier. Ions of identical mass are then captured
 132 by multiple Faraday cups, each positioned to capture specific masses (Fig. 1). The ion
 133 current flowing through the resistor of the cups producing a certain voltage serves as an
 134 output for the computer system, which converts relative signal strengths to a heavier
 135 isotope / lighter isotope ratio.

136



137

138 Fig. 1: Diagrammatic representation of dual inlet and continuous flow isotope ratio mass
 139 spectrometry (IRMS) analysis system.

140

141 There are two types of inlet system: dual-inlet (DI) and continuous-flow (CF) (Fig. 1).
 142 In either case, the inlet system introduces pure gases (e.g. CO₂, H₂, N₂, CH₄) into the
 143 IRMS via thin capillary tubes, which enable a constant viscous flow of gas molecules,
 144 ensuring no isotopic fractionation occurs prior to measurements. In a DI system, the

145 reference and sample gases are kept in separate bellows, keeping both gases under the
146 same pressure and from where they flow either into the ion source of a mass
147 spectrometer or to a waste line via a change-over valve (typically, 5 to 10 pairs of
148 sample and reference gas isotope ratio measurements are made for each sample) (Carter
149 and Barwick, 2011), allowing high precision isotope measurements of 0.01 ‰ for $\delta^{13}\text{C}$
150 and 0.03‰ for $\delta^{18}\text{O}$ in air for gaseous samples (Sulzman, 2007). In the CF inlet system,
151 the analyte CO_2 (sample or reference) is carried in a constant helium stream through a
152 gas chromatographic (GC) column or trap. Each sample gas is typically introduced only
153 once and followed (or preceded, depending on the analysis setting) by the introduction
154 of a reference CO_2 gas. Although, the CF-IRMS measurements can be less precise
155 (0.01-0.21 ‰ for $\delta^{13}\text{C}$ and 0.03-0.34 ‰ for $\delta^{18}\text{O}$; see decision tree diagram, section
156 3.5), its great advantage is on-line (automated) sample preparation. The CF-IRMS
157 instrumentation allows processing of a sample size from 100 up to 300 mL and enables
158 faster sample throughput, which can significantly reduce the analysis costs.

159 ***3.3 Measuring the stable isotope composition of CO_2 with LAS***

160 Laser-based spectroscopy (LAS) is the most convenient technique for *in-situ* trace gas
161 analysis, enabling CO_2 concentration and stable isotope analysis/measurements with
162 higher measuring frequency and reduced costs (Bahn et al., 2009 and Marron et al.,
163 2009).

164 In contrast to IRMS, LAS does not measure the isotope ratios but the mixing ratios of
165 individual isotopologues, e.g., $^{12}\text{CO}_2$ and $^{13}\text{CO}_2$. The working standards should
166 therefore bracket the expected mixing ratios of both isotopologues.

167 During the past 25 years, laser absorption spectroscopic techniques have become widely
168 commercially available (Tittel et al., 2013) and are used by a growing number of isotope
169 researchers for significant advances in their own field of research (Kerstel and
170 Ginafrani, 2008). A combination of measurement techniques appropriate to a particular
171 question will normally ensure the most robust results. In forest research, LAS
172 instruments are most effectively used in combination with micrometeorological
173 techniques, providing new tools for in depth investigation of the isotope exchange in
174 ecosystems (Aouade et al., 2016; Griffis et al., 2007; Griffis et al., 2008; Griffis et al.,
175 2010; Midwood and Millard, 2011; Munksgard et al., 2013; Santos et al., 2012; Sturm
176 et al., 2012; Wada et al., 2016; Wehr and Saleska, 2015; Wehr et al., 2016; Wehr et al.,
177 2017 and Wingate et al., 2010). CO₂ analysis in the field requires a compact, low
178 power, portable, robust, cost-effective and easy to use analytical system that, in some
179 cases, should enable sampling up to 10 times per second (Sturm et al., 2012). All these
180 factors should thus be carefully considered when measuring the concentration and
181 isotopic composition of CO₂ at remote locations.

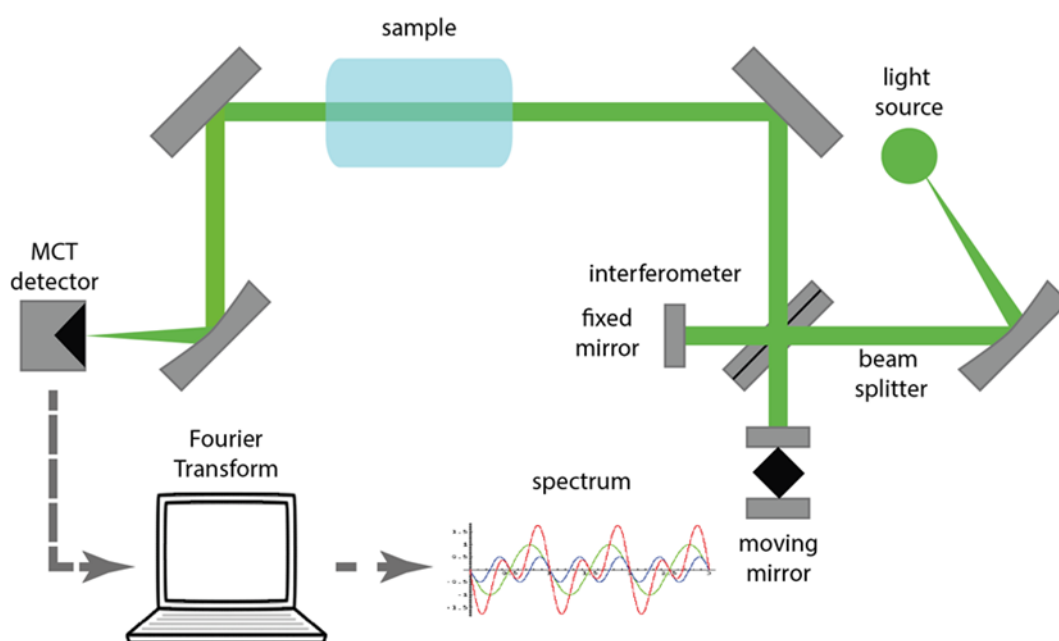
182 A key optical component for LAS is the commercial availability of high-performance
183 semiconductor lasers (Tittel et al, 2013). To put it simply, semiconductor lasers are
184 devices in the form of a diode that emits light in a certain narrow band wavelength.
185 Today, several LAS instruments are available, which differ in design, precision,
186 accuracy and sensitivity (Fig. 7). However, the most useful commercially available LAS
187 instruments for CO₂ concentration and stable isotopic measurements apply various
188 techniques, such as tunable diode laser absorption (TDLAS), quantum cascade laser
189 spectroscopy (QCLAS), cavity ring-down spectroscopy (CRDS) and off-axis cavity
190 enhanced absorption spectroscopy (OA-CEAS). The latter two are based on an external

191 cavity with high reflecting mirrors, with a reflectivity of $\geq 99.99\%$. This is also a
192 drawback of the technique (CRDS and OA-CEAS), since the highly reflective mirrors
193 can limit the usable wavelength range to some 10% of a central wavelength.
194 Furthermore, the laser beam quality is more critical than with other techniques (Sigrist
195 et al., 2008). Wen et al. (2012) provided a comprehensive comparison of the above-
196 mentioned LAS measurement techniques for water vapour isotope measurement. Their
197 work is the first systematic attempt to compare multiple LAS analytical instruments
198 (OA-CEAS, CRDS, QCLAS and TDLAS) to determine whether their calibration
199 methods are truly transferrable from one to another. Instruments based on these
200 techniques have been reported to operate with precisions of ± 0.04 to 0.25 ‰ for $\delta^{13}\text{C}$
201 and ± 0.05 to 2.0 ‰ for $\delta^{18}\text{O}$ (Barker et al., 2011; Wen et al., 2013; Xia et al. 2016) for
202 field measurements and thus approaching the ± 0.01 ‰ levels reported for IRMS in
203 several laboratories (Mortazavi and Chanton, 2002; Griffith et al., 2012 and van
204 Geldern et al., 2014)

205 *3.3.1 Fourier-transform infrared spectroscopy (FTIR)*

206 FTIR spectroscopy uses broadband infrared radiation from a blackbody light source that
207 covers the entire infrared spectrum simultaneously. In FTIR (Fig. 2) spectroscopy, the
208 source radiation is modulated by a Michelson interferometer (precisely measures the
209 wavelength of optical beams through the creation of interference patterns) and all
210 optical frequencies are recorded simultaneously in the measured interferogram (Griffith
211 et al., 2012). Fourier transform (a mathematical process) is required to convert the raw
212 data (intensity to frequency domain) into the actual spectrum. The method requires no
213 sample preparation other than optional drying of the sample and may be applied directly
214 to ambient air samples (Esler et al., 2000). Current FTIR spectrometers offer precise

215 quantification of a wide range of analytes for concentrations down to single-digit ppb
 216 levels and are now available as integrated and relatively compact units compared to the
 217 complex and bulky units offered in the past (Flores et al., 2017; Griffith et al., 2012;
 218 Griffith, 2018; Hammer et al., 2012 and McDonagh et al., 2008). Furthermore, in situ
 219 FTIR spectrometers record and store a broadband absorption spectrum, from 1800-5000
 220 cm^{-1} for each measurement. The recorded spectra are analysed online by non-linear least
 221 squares fitting of sections of the measured spectrum with a modelled spectrum
 222 calculated from the HITRAN database (Gordon et al., 2017; Hill et al., 2016; Rothman
 223 et al., 2013) of absorption line parameters. The theoretical spectrum is calculated by
 224 MALT (multiple atmospheric layer transmission) as described elsewhere (Griffith et al.,
 225 2012).
 226



227
 228 Fig. 2: Schematic illustration of fourier-transform infrared spectroscopy (FTIR) sketched
 229 following the example of Glewen (2007). In FTIR spectroscopy, IR radiation that has been

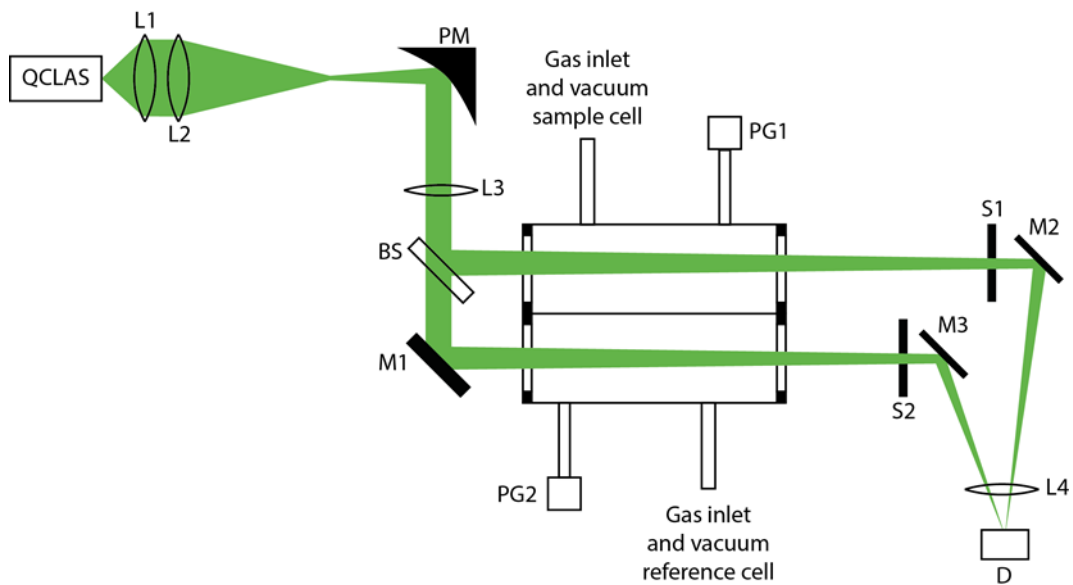
230 modulated is passed through the sampling area and is detected by a highly sensitive mercury
231 cadmium telluride (MCT) detector.

232

233 3.3.2 *Quantum cascade laser spectroscopy (QCLAS)*

234 QCLAS are semiconductor lasers and were first demonstrated in the nineteen nineties
235 by Faist et al. (1994). QCLAS (Fig. 3) offers real-time high-precision measurement of
236 mixing ratios of the individual CO₂ isotopologues using infrared absorption
237 spectroscopy with a pulsed, room-temperature quantum cascade laser (Nelson et al.,
238 2008 and Tuzson et al., 2008). QCLAS systems do not require special sample
239 preparation and are particularly attractive because of their stable single mode spectral
240 output, high power and because they offer a significant advantage for field deployment
241 due to real-time continuous in situ measurement (Saleska et al., 2006). With the
242 progressive development of a specialized QCLAS in the late 2000s, researchers (Nelson
243 et al., 2008 and Tuzson et al., 2008) have been able to do competent CO₂ isotope
244 monitoring. Their QCLAS scanned across three spectral lines (near 2310 cm⁻¹),
245 quantifying three CO₂ isotopologues: ¹²C¹⁶O₂, ¹³C¹⁶O₂ and ¹⁶O¹²C¹⁸O. In another study,
246 Saleska et al. (2006) used a pair of CO₂ spectral lines near 2311 cm⁻¹ (2311.399 cm⁻¹ for
247 ¹³C¹⁶O₂ and 2311.105 cm⁻¹ for ¹²C¹⁶O₂). Wehr et al. (2013) used cryogen-free,
248 continuous-wave QCLAS for eddy covariance measurement of the net ecosystem
249 exchange of CO₂ isotopologue molar mixing ratios (¹³C¹⁶O₂, ¹⁸O¹²C¹⁶O, and ¹²C¹⁶O₂).
250 They collected the data of real-time isotopic CO₂ measurements over the 2011 growing
251 season (from May to October 2011) in a temperate deciduous forest dominated by trees
252 such as red oak and red maple, located at the Harvard Forest in Petersham,
253 Massachusetts, USA. Similarly, Sturm et al. (2012) used QCLAS and the eddy

254 covariance method to measure isotope fluxes of $^{12}\text{C}^{16}\text{O}_2$, $^{13}\text{C}^{16}\text{O}_2$ and $^{16}\text{O}^{12}\text{C}^{18}\text{O}$ above a
 255 forest canopy. The QCLAS system was established at the Swiss national air pollution
 256 monitoring site in the beech dominated forest in the Lägeren mountains (Switzerland).
 257



258
 259 Fig. 3: Schematic illustration of quantum cascade laser spectroscopy (QCLAS) consisted of
 260 parabolic mirror (PM), beam splitter (BS), mirrors (M), shutter (S), pressure gauge (PG),
 261 detector (D) and lenses (L1 and L2). The QCLAS system was sketched following the example
 262 of Castrillo et al. (2007).
 263

264 3.3.3 Tunable Diode Laser Absorption Spectroscopy (TDLAS)

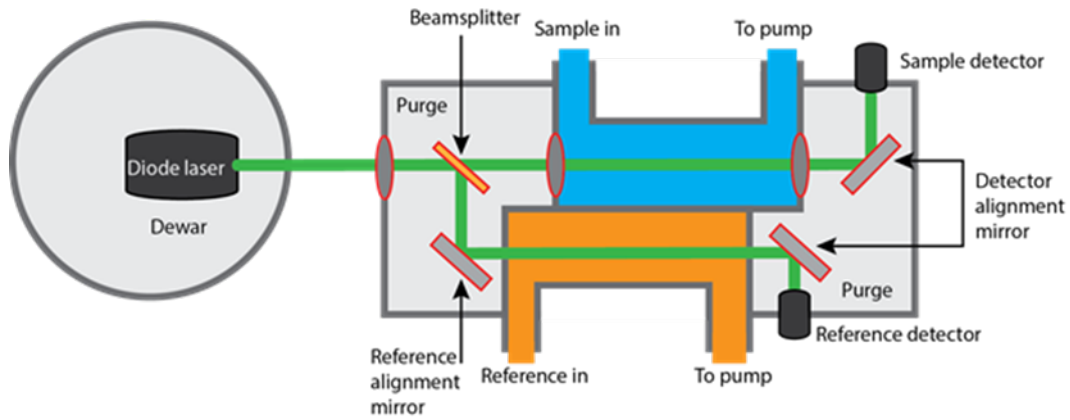
265 TDLAS is a commonly used LAS instrument for quantitative measurements in gaseous
 266 media and is gaining in popularity for measuring the mole fraction and stable isotopic
 267 composition of CO_2 in air in studies of biosphere-atmosphere gas exchange (Schaeffer
 268 et al., 2008). TDLAS measures the absorption of infrared energy, which is proportional
 269 to molecular density, following Beer's law (Sulzman, 2007). The analytical instrument
 270 utilizes semiconductor lasers to detect a variety of different trace gases, from oxygen in

271 the near infrared range to carbon dioxide and carbon monoxide in the short-wavelength
272 infrared range. This measurement technique enables the miniaturization of transmission
273 and receiving units, providing highly sensitive, quantitative measurements with fast
274 response times without the need for frequent calibration (Shuk and Jantz, 2015).
275 TDLAS usually scans over an isolated absorption line of the chemical species under
276 investigation using a single narrow laser line. To achieve the highest selectivity,
277 analysis is done at low pressure, whereby the absorption lines are not substantially
278 broadened by pressure (Werle, 1998). One of the most important applications of
279 TDLAS in atmospheric measurements has turned out to be their use in combination
280 with a multi-pass cell with path lengths of 100 m or more (Werle et al., 2004).

281 TDLAS measures the mixing ratios of stable isotopes of carbon dioxide in the air (e.g.,
282 the isotopologues, $^{12}\text{C}^{16}\text{O}_2$, $^{13}\text{C}^{16}\text{O}_2$ and $^{16}\text{O}^{12}\text{C}^{18}\text{O}$) by comparing the infrared
283 absorption of sample and reference gases in a specific absorption line of the spectrum
284 (Santos et al., 2012). However, measuring the stable isotope composition with TDLAS
285 requires high mole fraction measurement accuracy for a single isotope, although
286 TDLAS has been shown to be capable of effective, accurate measurement even when
287 losing ~95% of the original signal in a dusty environment (Shuk and Jantz, 2015). The
288 majority of reported field campaigns applications (Bowling et al., 2003, Marron et al.,
289 2009, Santos et al., 2012 and Wingate et al., 2010) were conducted with the
290 instruments, TGA200 and TGA200A (Campbell Scientific, Inc., Logan, UT, USA) (Fig.
291 4), based on the original patented design developed by Edwards, Kidd, and Thurtell at
292 the University of Guelph (Edwards et al., 1994). For CO_2 isotopologue measurement the
293 TGA200 and TGA200A analytical instruments can be tuned to adsorption lines between
294 2293 and 2311 cm^{-1} . Common to all is a combination of the LAS measurement

295 technique with the use of micrometeorological instruments such as temperature and
296 moisture sensors. A successful use of a TDLAS field campaign for ecosystem-
297 atmosphere CO₂ exchange studies was conducted by Bowling et al. in 2003. They
298 measured the carbon isotope content of CO₂ at atmospheric mole fractions and isotopic
299 abundance of $\delta^{13}\text{C}$. The ability of the instrument to measure isotope ratios of $\delta^{13}\text{C}$ was
300 tested outdoors in a grassland and compared to standard laboratory based IRMS. In
301 addition, Wingate et al. (2010) carried out a comprehensive field campaign in a nearly
302 homogenous maritime pine forest, while designing a multi-inlet sampling system
303 automatically to select and measure the CO₂ isotope composition and environmental
304 conditions in the vertical atmospheric profile below, within and above the canopy, in
305 open soil chambers and a closed branch chamber. In a similar experimental setup,
306 Santos et al. (2012) used a TDLAS instrument in near-continuous measurement to study
307 the CO₂ stable isotopic exchange near the floor of a temperate deciduous forest. Marron
308 et al. (2009) recorded the temporal variability of $\delta^{13}\text{C}$ composition of CO₂ efflux
309 released by forest soil at different time scales and showed that TDLS can also be useful
310 at an ecosystem level. In another study, Schaeffer et al. (2008) conducted the first multi-
311 year analysis of TDLAS instrument performance for measuring CO₂ isotopes in the
312 field (high-altitude subalpine coniferous forest at Niwot Ridge AmeriFlux). Air was
313 sampled from five to nine vertical locations in and above the forest canopy every ten
314 minutes for 2.4 years. Von Sperber et al. (2015) researched the influence of soil
315 moisture, soil particle size, litter layer and carbonic anhydrase on the isotopic
316 composition of soil-released CO₂ and H₂O in soil column experiments under
317 laboratory conditions. They used a TGA200 instrument in their research, which was

318 tuned to adsorption lines at 2308.171 cm^{-1} for $^{13}\text{C}^{16}\text{O}_2$, 2308.225 cm^{-1} for $^{12}\text{C}^{16}\text{O}_2$ and
 319 2308.416 cm^{-1} for $^{16}\text{O}^{12}\text{C}^{18}\text{O}$.
 320



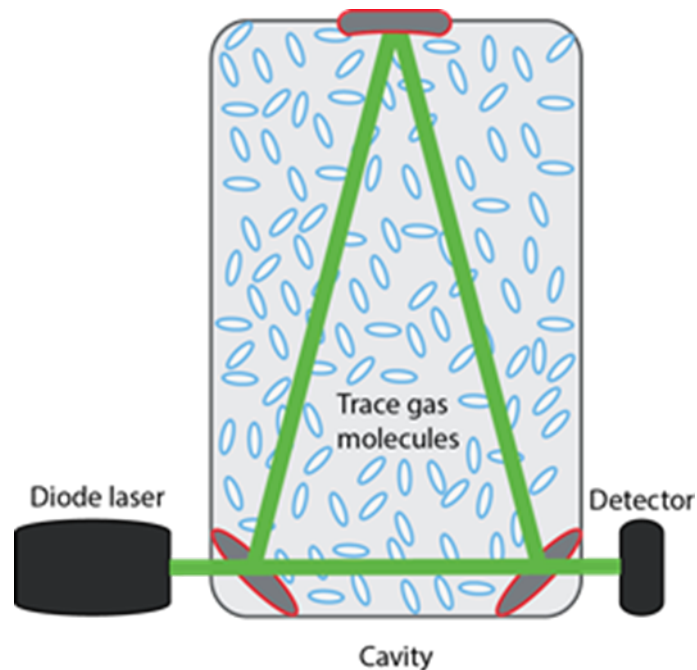
321
 322 Fig. 4: Schematic illustration of tunable diode laser absorption spectroscopy (TDLAS).
 323 Sketched following the example of Campbell Scientific, Inc., Logan, UT, USA.
 324

325 *3.3.4 Cavity Ring-Down Spectroscopy (CRDS)*

326 CRDS is a spectroscopic measurement technique for detecting atmospheric trace gases
 327 and was pioneered by O’Keefe and Deacon (1988). A typical CRDS setup involves an
 328 optical cavity made from two (O’Keefe and Deacon, 1988) or three (Fig. 5) (Morville et
 329 al., 2005 and Paldus et al., 1998) highly reflective mirrors (reflectance $>99.999\%$), in
 330 which photons propagate for a prolonged time (Rao, 2012). However, a three-mirror
 331 cavity provides superior signal to noise compared to a two-mirror cavity that supports a
 332 standing wave (Picarro, Inc., Santa Clara, CA, USA). CRDS spectroscopy is a direct
 333 absorption technique, which can be performed with pulsed or continuous light sources
 334 and has a significantly higher sensitivity than obtainable in conventional absorption
 335 spectroscopy (Berden et al., 2000). Light is coupled into the cavity through one of the
 336 mirrors and light leaking out of the cavity is detected, i.e., the technique is based on

337 measurement of the rate of absorption rather than the magnitude of absorption of a light
338 pulse confined in a closed optical cavity with a high-quality factor. The advantage over
339 normal absorption spectroscopy is a result of the intrinsic insensitivity to light source
340 intensity fluctuations, the extremely long effective path lengths (> 10 km) that can be
341 realized in stable optical cavities and time-based measurements (Berden et al., 2000).
342 Like other analysers, CRDS instruments are designed for very sensitive gas absorption
343 measurements and have volumes of tens to hundreds of millilitres (Crosson, 2008 and
344 Waechter et al., 2010).

345



346

347 Fig. 5: Schematic illustration of a cavity ring-down spectroscopy (CRDS) analyser cavity
348 showing how a ring down measurement is carried out in a three-mirror cavity (sketched
349 following the example of Picarro, Inc., Santa Clara, CA, USA). The gas sample is led into in a
350 three highly reflective mirror ($R \sim 0,9999$) cavity, shown in the figure above, to support a
351 continuous traveling light wave.

352

353 CRDS instruments have been commercially available for decades. Recently, cavity ring-
354 down spectroscopy has been successfully employed in carbon dioxide detection.
355 Munksgaard et al. (2013) described in detail the method and application of field-based
356 CRDS measurement techniques of $\delta^{13}\text{C}$ in soil respired CO_2 , while comparing the
357 instrument precision with that of continuous flow–isotope ratio mass spectrometry (CF-
358 IRMS). They used a CRDS analyser (model G2012-i; Picarro, Inc.) in two modes,
359 firstly for continuous analysis of soil-respired CO_2 drawn directly from a soil chamber
360 into the analyser at a controlled rate and, secondly, for batch analysis of carbon dioxide
361 in sequentially sampled gas bags from a soil chamber. CRDS measurements of $\delta^{13}\text{C}$ and
362 CO_2 were performed at 1 Hz. The instrumental precision of individual $\delta^{13}\text{C}$
363 determinations was $<0.3\text{‰}$ for a 5-min integration time (1-Sigma Standard Deviation,
364 1SD), drift was $<2\text{‰}$ over 24 h. According to Picarro, Inc., 5-minute averaged
365 precision is often used in industry and is a useful averaging time for many types of
366 measurements in scientific applications. The precision is the 1SD of 5-minutes
367 averages, obtained over at least 60 minutes of measurement. This means that it obtains
368 at least 12 average values of five minutes length. A 1SD of 0.3‰ means that 67% of
369 these 5-minute averages are scattered around the mean value $M \pm 0.3\text{‰}$. To have a
370 higher confidence, you would need to take the 2-Sigma Standard Deviation, in this case
371 95% of the 5-min averages will fall within a band of $M \pm 0.6\text{‰}$. The drift specification
372 is based on peak-to-peak differences over a measurement period of at least 24 hours.
373 The analytical technique developed in their study demonstrated an acceptable accuracy
374 and precision for the determination of $\delta^{13}\text{C}$ values in soil-respired CO_2 in field
375 campaigns. The CRDS analyser (model G2131-i; Picarro Inc.) can measure the $^{13}\text{CO}_2$
376 stable isotope abundance by measuring two independent spectral absorption lines in the

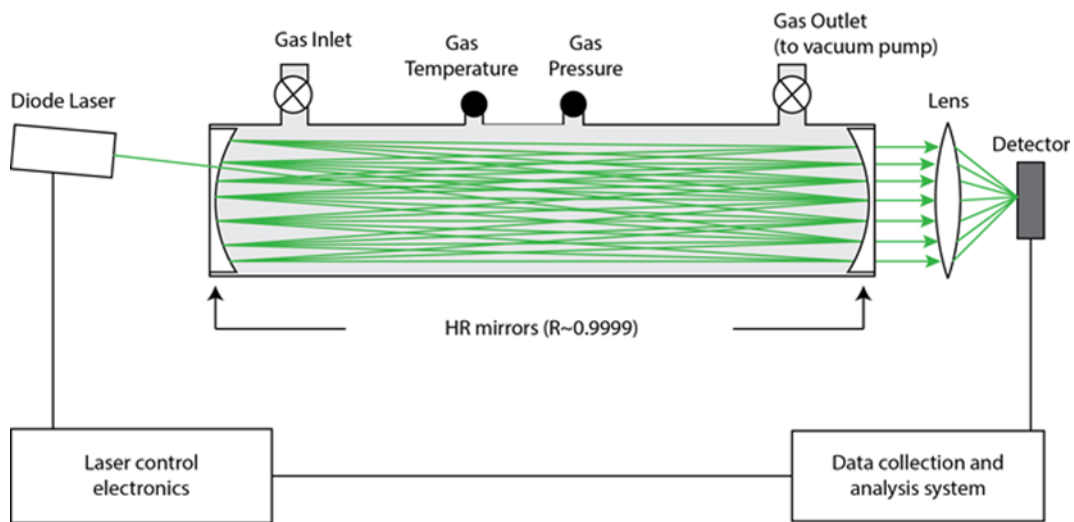
377 near-infrared region of the spectrum, including one for $^{12}\text{C}^{16}\text{O}_2$ at 6251.760 cm^{-1} and
378 one for $^{13}\text{C}^{16}\text{O}_2$ at 6251.315 cm^{-1} (Dickinson et al., 2017). The precision of the system
379 has been reported to be better than 200 ppb for $^{12}\text{C}^{16}\text{O}_2$ and 10 ppb for $^{13}\text{C}^{16}\text{O}_2$ for a 30-
380 s measurement as the measuring time increases (Maher et al., 2014). In another field
381 campaign Albanito et al. (2012) deployed a CRDS analyser (model G1101-i; Picarro,
382 Inc.) for continuous measurement of two CO_2 isotopologue mixing ratios ($^{12}\text{C}^{16}\text{O}_2$ and
383 $^{13}\text{C}^{16}\text{O}_2$) and isotopic signature ($\delta^{13}\text{C-CO}_2$) by connecting the CRDS analyser with dual-
384 chambers inserted into the soil to a depth of approximately 2-3 cm in semi-managed
385 Mediterranean pine forest. Samples were collected and analysed throughout daylight
386 hours and separated into those collected in the morning and afternoon to detect any
387 short-term temporal changes in CO_2 flux (from roots, litter/humus and old soil organic
388 matter) and isotopic signature ($\delta^{13}\text{C-CO}_2$). They used a multichannel gas sampling
389 control system programmed to perform routine analysis. In a different survey, Dubbert
390 et al. (2014) presented the first data set on daytime cycles (morning and afternoon
391 measurements) of direct estimates of the isotopic composition of transpired water
392 vapour in key environmental periods in a Mediterranean climate: spring wetness,
393 summer drought and the beginning of a wet and cold autumn in cork-oak trees (*Quercus*
394 *suber*). Fluxes and the isotopic composition of cork-oak transpiration were measured
395 using a CRDS instrument (model L2120-i; Picarro, Inc.) in combination with custom-
396 built branch chambers in an open gas exchange system. In another field campaign
397 Jochheim et al. (2017) deployed an isotopic analyser based on wave-length-scanned
398 cavity ring-down spectroscopy (model G1101-i; Picarro, Inc.). The CRDS instrument
399 was used to detect seasonal dynamics in beech and pine forest soils at different soil
400 depths, while connected via a 16-position valve (VALCO STF) for the detection of

401 $\delta^{13}\text{C-CO}_2$, consecutively for each channel. The precision of the isotopic analyser for
402 $\delta^{13}\text{C}$ was $< 0.3\text{‰}$. In such a layout - a sequence of 16 channels was achieved within 80
403 minutes, resulting in 18 measurement cycles per 24 h.

404 3.3.5 Off-axis Cavity Enhanced Absorption Spectroscopy (OA-CEAS)

405 The off-axis design eliminates optical feedback from the cavity to the light source. Such
406 an arrangement causes the light to be many times reflected by the mirrors and it fills the
407 whole volume of the cavity (Nowakowski et al., 2009). For example, for a cell
408 composed of two 99.99% reflectivity mirrors spaced at 25 cm, the effective optical path
409 length is 2500 meters (ABB - Los Gatos Research, San Jose, CA, USA). The use of
410 OA-CEAS, which utilizes a high-finesse optical cavity as an absorption cell, is shown in
411 Fig. 6.

412



413

414 Fig. 6: Schematic diagram of an instrument based on OA-CEAS (sketched following the
415 example of ABB - Los Gatos Research, San Jose, CA, USA). The gas sample is passed
416 continuously through the cavity while the off-axis laser beam bounces multiple times between
417 the highly reflective (HR) ($R \sim 0.9999$) mirrors.

418

419 The method was introduced by Paul et al. (2001) and their paper clearly explains the
420 basic principles. However, a fundamental problem with this technique is that the higher
421 the finesse resonant optical cavity, the narrower the transmission mode envelope of the

422 cavity, and the more difficult it becomes to inject light into the cavity. OA-CEAS has
423 advantages due to its enhanced sensitivity, high mechanical robustness and relatively
424 simple optical configuration, which make it suitable for long-term measurements in the
425 field (Gupta, 2012). Sprenger et al. (2017) reported that OA-CEAS analytical
426 instruments use the absorption of a near-infrared laser beam by molecules (i.e.,
427 isotopologues) in a gaseous sample in a high-finesse optical cavity (Crosson, 2008; Baer
428 et al., 2002). Directing the laser beam off-axis allows spatial separation of the multiple
429 reflections within the cavity, (Paul et al., 2001), which results in fully resolved OA-
430 CEAS absorption spectra (ABB - Los Gatos Research). Other associated LAS
431 measurement techniques, such as CRDS, have a disadvantage when it comes to
432 obtaining data in high temporal resolution. The mentioned constraints of CRDS favour
433 OA-CEAS instruments when performing high-quality measurements of relevant trace
434 gases (e.g., carbon dioxide, carbon monoxide) in different ecosystems (forest, caves, sea
435 etc.) (Arévalo-Martínez et al., 2013). While OA-CEAS instruments are now being
436 routinely used in terrestrial ecosystems continuously to measure, e.g., for analysis of the
437 stable isotopes of water ($\delta^2\text{H}$ and $\delta^{18}\text{O}$) in different soil types (Orlowski et al., 2016),
438 there are not many published research papers using OA-CEAS instruments for carbon
439 dioxide isotope composition measurements in forest field campaigns. However, here we
440 present two examples of successful monitoring of carbon dioxide using OA-CEAS
441 instruments. In an effort to monitor leakage from underground CO_2 storage,
442 (McAlexander et al., 2011) tested a field-deployable analyser capable of rapidly
443 measuring the CO_2 mixing ratio and carbon isotope $\delta^{13}\text{C}$ values. The analyser was
444 interfaced with a multipoint inlet unit to allow autonomous sampling from multiple
445 locations. In the mentioned study, they used an OA-CEAS isotope analyser from ABB -

446 Los Gatos Research to measure simultaneously both CO₂ concentration and carbon
447 isotope composition. In another study, (Mahesh et al., 2015) tested a greenhouse gas
448 analyser instrument (model GGA-24EP, ABB - Los Gatos Research), which used an
449 OA-CEAS analyser with the objective of generating a long-term record of
450 measurements of CO₂ and CH₄ concentrations conforming to standards set by the World
451 Meteorological Organization. A research campaign using corrected observations over
452 12 months revealed the role of wind velocity and anthropogenic emissions, as well as
453 seasonal variations in the ambient concentrations of CO₂ and CH₄ gases near the
454 surface.

455 **3.4 Combination of micrometeorological techniques and stable isotope analysis**

456 Several different measuring techniques for stable isotope and concentration analysis of
457 CO₂ in forest ecosystem are available. Researchers usually choose the methods that
458 most reliably deliver the results researchers are seeking. Many researchers (Aouade et
459 al., 2016; Wada et al., 2016, 2017; Stropes, 2017; Wen et al., 2016) combine
460 micrometeorological measurements and advanced stable isotope analysis. Field-scale
461 applications of this combined technology are now under development. IRMS and LAS
462 analysers can be used in combination with micrometeorological techniques in chamber
463 measurements, eddy covariance measurements or for vertical profile measurements of
464 trace gas (e.g., CO₂) concentrations measured from tall and flux towers monitoring
465 boundary layer mixing processes and trace gas exchange between the atmosphere,
466 surface and plant/forest communities (Griffith et al., 2012). This combination of
467 techniques allows very precise and frequent/continuous measurements of CO₂
468 components at the ecosystem scale and brings new insights into the mechanisms

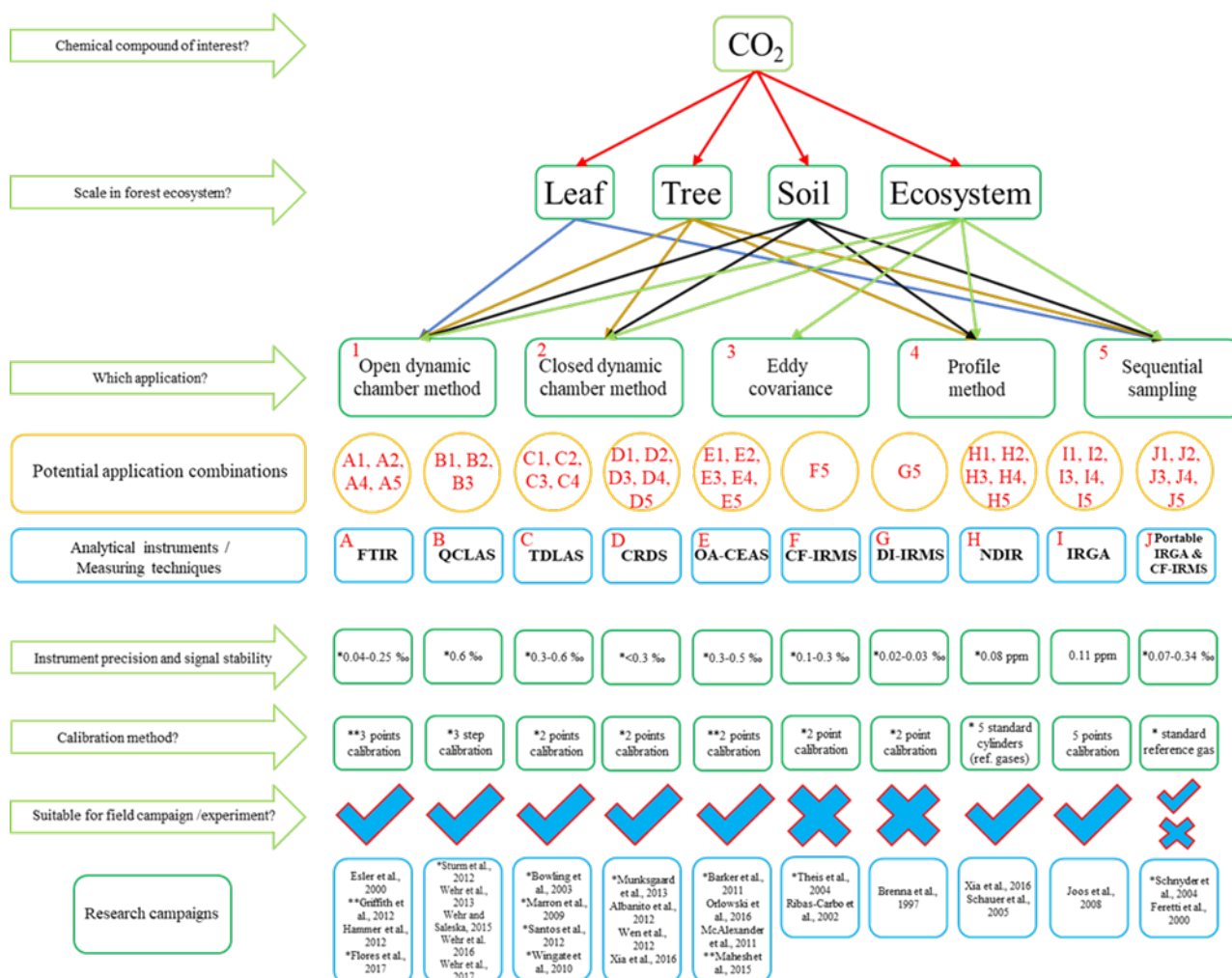
469 governing biochemical cycles in ecosystems (Stropes, 2017). The choice of instrument
470 for a particular experiment depends not only on cost and measurement stability but also
471 on the time to get the advantage of the required precision. For example, if used for eddy
472 covariance measurements, then sampling rates higher than 5 Hz are required, while
473 random noise is not so much of a problem and can be filtered. If measuring sample bags
474 of CO₂ isotopologues, then high precision may be required in less than 30 s and an
475 analytical instrument with the same precision that takes 5 minutes may not be
476 appropriate. Furthermore, researchers should consider that sample storage in sample
477 bags provides acceptable results only for a short time (up to 10 days of storage),
478 because evaporitic isotopic enrichment might occur with samples stored for up to 6
479 months (Hendry et al., 2015). Power consumption is another important requirement that
480 might necessitate a particular choice of instrument. When reviewing the power
481 consumption of the analytical instruments, we found that, in most cases, recently
482 published research studies do not provide this information. Nevertheless, by comparing
483 a number of studies considered in our paper, we can assume that there are significant
484 differences between the instruments in power consumption. For example, the whole
485 QCLAS system (including the pumps) would need as much as 2000 W of power to
486 operate (Sturm et al., 2012), which is approximately 600W more than OA-CEAS or CF-
487 IRMS systems. By contrast, IRGA instruments require only about 20-35 W of power to
488 operate, while providing robust data sets. These analytical systems provide the lowest
489 power costs and smallest carbon footprint of all gas systems available. However, their
490 scope of analysis is consequently smaller and less demanding. Another important
491 consideration for making reliable field measurements is the ease of calibration of the
492 analytical instruments, which is a requirement that impacts on the quality/accuracy of

493 analysis. Assume that there is a selection of instruments (one or several) individually
494 measuring each of the most abundant CO₂ isotopologues. Each isotopologue is usually
495 calibrated independently after decomposing the standard's total CO₂ into its component
496 isotopologue mole fractions using the methods discussed by Flores et al. (2017), Griffis
497 (2013), Griffith (2018), Tans et al. (2017) and several others. How frequently such
498 calibrations need to be repeated depends on the individual instrument. In summary, it
499 can be said that each approach has its advantages, disadvantages and logistical
500 challenges. Hence, even though experimental approaches may differ from each other,
501 most of the described combinations can be considered reliable for carbon isotope
502 fractionation investigations.

503 **3.5 Decision tree classifier: decision making process**

504 CO₂ is a crucial element of interest in ecosystems. Analytical instruments and
 505 application techniques for CO₂ (concentration and stable isotopologues of CO₂) are
 506 discussed in detail. To ease the decision on selection of the suitable application for the
 507 desired ecosystem scale (leaf, tree, soil or whole ecosystem level), we prepared a
 508 decision tree (Fig. 7) on up-to-date and relevant application/measuring techniques. Each
 509 application option is supported by selected research campaigns and references.

510



511

512 Fig. 7: Schematic diagram of decision tree (DT). The result of a DT is a set of potential
 513 application combinations, which are presented with an alphanumeric combination shown in

514 circles above. For example, alphanumeric combination (A1) indicates that an FTIR analytical
515 instrument can be used in combination with an open dynamic chamber method.

516 **4. Conclusions and Outlook**

517 The need to meet increasingly stringent research, environmental and legislative
518 requirements has led to the development of IRMS and LAS analytical techniques to
519 measure concentrations and stable isotopologues of carbon dioxide. There are many
520 reasons why carbon dioxide isotopologues offer great added value in studies on the
521 carbon cycle in a natural environment. One is that they enable insight into the origins of
522 the chemical species/elements (C, N...), as well as their uses as tracers. The other is that
523 high-frequency measurements may ambiguously explain a particular ecosystem process
524 (Aelion et al., 2009). IRMS and LAS analytical systems offer high precision for
525 measuring very small changes in isotope concentrations in selected natural
526 environments. van Geldern et al. (2014) noted that the monitoring data set would not
527 have been as complete if only IRMS analyses had been used. LAS data revealed a much
528 more intense dynamic, with fast changing $\delta^{13}\text{C}$ values. In the past, researchers relied on
529 measurements of concentrations of the chemical elements/compounds of interest in the
530 specific environment. This was not always successful and often led to uncertainty
531 because determination of stable isotopologues of carbon dioxide constitutes a challenge
532 in several ways, since the application/measurement technique needs to be sufficiently
533 sensitive and specific to detect the chemical species. It is important to highlight that
534 instrument noise can limit the instrument's ability to detect small changes in the
535 concentration of isotopes in ecosystems over a given time period. One option is to use
536 longer averaging periods, which can reduce some instrument noise. Furthermore,
537 Stropes (2017) stressed that statistical approaches, such as Allan deviation analysis, can

538 be used to evaluate instrument precision and its relationship with the averaging time.
539 This approach has successfully been used in some previous studies to evaluate the
540 precision of isotope ratio measuring systems (Tuzson et al., 2011 and Sturm et al.,
541 2012). This analysis could provide means to find the optimum averaging time interval
542 with the least deviation, and therefore most precision, in concentration signals for a
543 sampling system.

544 CO₂ analysers are not equally sensitive to the isotopologues of CO₂. For example, LAS
545 measurement techniques, which measure an absorption line from the most abundant
546 CO₂ isotopologue ¹²C¹⁶O₂, are blind to all the minor isotopologues of CO₂ (Tans et al.,
547 (2017). Furthermore, NDIR instruments are much more complicated in their response to
548 the various minor isotopologues of CO₂. Most NDIR analysers use an optical band-pass
549 filter to limit the wavelengths of light reaching the detectors. These filters often exclude
550 part of the absorption bands of the minor isotopologues (e.g., Tohjima et al., 2009) but
551 are more sensitive to the ¹³C¹⁶O₂ lines within the passband because absorption of the
552 much stronger ¹²C¹⁶O₂ lines is partially saturated. The width and shape of the
553 transmission window of the filter are generally not identical between analytical
554 instruments. Tohjima et al. (2009) found significant differences in sensitivity to the
555 minor isotopologues between different NDIR analysers. Karlovets et al. (2018) reported
556 that, in spite of their low natural abundances, the ¹³C minor isotopologues (in particular
557 ¹⁶O¹³C¹⁸O, with a natural abundance less than 4.5×10⁻⁵) contribute importantly to small
558 residual opacity. Multiple minor isotopologues of CO₂ have very low terrestrial
559 abundances according to the spectroscopic database HITRAN (10⁻⁶ and 10⁻⁷ for
560 ¹⁶O¹³C¹⁷O and ¹²C¹⁷O₂, respectively) so their contribution to the m/z 46 signal is
561 considered negligible. This is not the case for m/z 45 signal or the ¹³C analysis, in which

562 the $^{16}\text{O}^{12}\text{C}^{17}\text{O}$ makes up about 7.27% ($=0.0008/0.011$) of the total intensities. In order to
563 determine how much of the m/z 45 signal is due to ^{13}C , we need to know how much of
564 it is due to ^{17}O . This is done by assuming that the ratio of ^{18}O to ^{17}O is constant in all
565 mass-dependent processes that result in isotope fractionation. (W. M. Keck Foundation
566 Laboratory for Environmental Biogeochemistry, [https://www.kfleb.org/introduction-to-](https://www.kfleb.org/introduction-to-isotope-analyses)
567 [isotope-analyses](https://www.kfleb.org/introduction-to-isotope-analyses); last access: 01 August 2019).

568 The accuracy of this calculation of concentrations (LAS analysis results) depends on
569 knowledge of the instrumental laser line width and shape, and the molecular line
570 parameters, including line strength, pressure and temperature dependence. For most
571 trace gases of interest, the positions, strengths, widths and temperature dependences of
572 relevant absorption lines are available in the HITRAN database (Gordon et al., 2017;
573 Hill et al., 2016; Rothman et al., 2013) and in CDSDB databank (Tashkun et al., 2015;
574 Tashkun et al., 2019). HITRAN is an acronym for high-resolution transmission
575 molecular absorption database and is available on the website of HITRANonline:
576 <https://hitran.org/> or HITRAN on the Web: <http://hitran.iao.ru/home> (last access: 01
577 August 2019). CDSDB is an acronym for Carbon Dioxide Spectroscopic Databank and is
578 available in HITRAN format as a single zipped ASCII file in the website of V.E. Zuev
579 Institute of Atmospheric Optics of the Siberian Branch of the Russian Academy of
580 Science: <ftp://ftp.iao.ru/pub/CDSDB-296> (last access: 01 August 2019). Comparisons of
581 new versions of the CDSDB with HITRAN line lists are published in a paper by Tashkun
582 et al. (2019). The basic underlying principles of a number of commercially available
583 measurement systems, together with some of their key characteristics, which may help
584 to inform their use in future research campaigns are reviewed in papers by Bowling et
585 al. (2003), Saleska et al. (2006), McAlexander et al. (2011), Guillon et al. (2012), Wen

586 et al. (2012), Griffis (2013), Rothman et al. (2013), Elliott et al. (2014), Tashkun et al.
587 (2015), Dickinson et al. (2017), Gordon et al. (2017), Tans et al. (2017), Griffith (2018),
588 Tashkun et al. (2019), and others.

589 As mentioned earlier, spectroscopic databases are partly devoted to use in atmospheric
590 retrieval models. These databases contain mainly, but not only, line-by-line spectra with
591 quantum number assignments and a number of other spectroscopic parameters, which
592 together are called a line list (Žak, 2017). For a successful measurement of
593 isotopologues of CO₂, all absorption lines in a given spectral region have to be
594 characterized, requiring high-resolution supporting data. There have been extensive
595 efforts by several research groups (Gordon et al. (2017); Tashkun et al. (2019); Huang
596 et al. (2017) and Jacquinet-Husson et al. (2016)) to expand the characterization of CO₂
597 isotopologues, from both experimental and theoretical standpoints, while
598 using/comparing different spectroscopic databases (e.g. HITRAN, CDSD, AMES and
599 GEISA). However, the LAS analysis uncertainty resulting from inconsistency hidden
600 among these spectroscopic databases for CO₂ isotopologues, is still a question (Pogány
601 et al., 2013). This question is well justified, since the intensity of most CO₂ IR
602 transitions in spectroscopic databases have >1% uncertainty. More importantly, for the
603 minor isotopologues, the uncertainty in the sample abundance is the result of intensity
604 uncertainties, which range from 1.5% for the more abundant species (¹³C¹⁶O₂) to 5% for
605 the less abundant ones (Toth et al., 2008). This is caused by inconsistency between the
606 intrinsic models used, namely the different effective dipole models (EDM) individually
607 fitted from different isotopologue experimental data. For example, Hovorka et al.
608 (2017) highlighted two main phenomena that perturb LAS measurements while
609 optimizing the data retrieval process for spectroscopic CO₂ isotopologue ratio

610 measurements: a.) interference between different molecular transitions (not necessarily
611 from the same molecule) b.) the different intensity temperature dependence of the two
612 transitions used for R (the ratio of the heavier over the lighter isotopologue) retrieval.
613 For a detailed review of potential LAS analysis uncertainty for isotopologues of CO₂,
614 see Ref. (Žak, 2017) and references therein.

615 The further development of analysers will surely help advance the ability to study plant,
616 canopy and ecosystem responses to climate change (Griffis, 2013). Advanced high
617 frequency stable isotope measurements provide great improvements over traditional
618 approaches and, in combination with micrometeorological measurements (see decision
619 tree diagram, Fig. 7), can trace the movement of CO₂ in ecosystems and the magnitude
620 of transportation in processes that exchange CO₂ (Griffis, 2013, Flanagan & Farquhar,
621 2014 and Riederer et al, 2015). For example, Wehr et al. (2017) combined these
622 approaches better to estimate stomatal conductance, transpiration and evaporation in a
623 temperate deciduous forest. Such approaches improve our understanding of carbon and
624 water cycling. Furthermore, the success of trace gas measuring techniques crucially
625 depends on the availability, sensitivity and performance of the analyser, combined with
626 appropriate detection schemes and spectroscopic databases. We have tried to highlight
627 the advantages and disadvantages of isotope measurement techniques throughout this
628 manuscript. Many technical aspects discussed in this review paper deserve deeper or
629 more thorough investigation. In other words, several topics could easily be extended to
630 full-length, independent papers. However, the core value of our review is to provide a
631 list of selected analytical instruments in a wide range of applications deployed in
632 terrestrial ecosystems, which we hope will be useful for the scientific community,
633 including IRMS and LAS laboratories. We believe that the new analytical instruments,

634 together with the challenges that remain, make this an exciting and rapidly developing
635 research field for years to come.

636 **Acknowledgements**

637 The authors acknowledge the financial support from the Slovenian Research
638 Agency (public tender "Promoting employment of young PhDs" in 2015 and
639 research core funding No. P4-0107, No. J4-5519, No. J4-8216 and No. Z4-8217). We
640 are thankful to anonymous reviewers for valuable comments and suggestions which
641 significantly improved the quality of the paper.

642 **References**

- 643 Aelion, C. M., Höhener, P., Hunkeler, D., Aravena, R., 2009. Environmental Isotopes in
644 Biodegradation and Bioremediation. CRC Press, p. 464.
645 <https://doi.org/10.1201/9781420012613>.
- 646
- 647 Albanito, F., McAllister, J.L., Cescatti, A., Smith, P. and Robinson, D., 2012. Dual-
648 chamber measurements of $\delta^{13}\text{C}$ of soil-respired CO_2 partitioned using a field-based
649 three end-member model. Soil Biol. Biochem., 47, 106-115.
650 <https://doi.org/10.1016/j.soilbio.2011.12.011>.
- 651
- 652 Aouade, G., Ezzahar, J., Amenzou, N., Er-Raki, S., Benkaddour, A., Khabba, S. and
653 Jarlan, L., 2016. Combining stable isotopes, Eddy Covariance system and
654 meteorological measurements for partitioning evapotranspiration, of winter wheat, into
655 soil evaporation and plant transpiration in a semi-arid region. Agricultural water
656 management, 177, 181-192. <https://doi.org/10.1016/j.agwat.2016.07.021>.
- 657
- 658 Arévalo-Martínez, D. L., Beyer, M., Krumbholz, M., Piller, I., Kock, A., Steinhoff, T.,
659 Körtzinger, A., Bange, H. W., 2013. A new method for continuous measurements of
660 oceanic and atmospheric N_2O , CO and CO_2 : performance of off-axis integrated cavity
661 output spectroscopy (OA-ICOS) coupled to non-dispersive infrared detection (NDIR).
662 Ocean Sci., 9, 1071-1087. <https://doi.org/10.5194/os-9-1071-2013>.
- 663
- 664 Bahn, M., Schmitt, M., Siegwolf, R., Richter A., Brüggemann, N., 2009. Does
665 photosynthesis affect grassland soil-respired CO_2 and its carbon isotope composition on

666 a diurnal timescale? *New Phytol.*, 182, 45-460. <https://doi.org/10.1111/j.1469->
667 [8137.2008.02755.x](https://doi.org/10.1111/j.1469-8137.2008.02755.x).

668

669 Barker, S. L., Dipple, G. M., Dong, F., and Baer, D. S., 2011. Use of laser spectroscopy
670 to measure the $^{13}\text{C}/^{12}\text{C}$ and $^{18}\text{O}/^{16}\text{O}$ compositions of carbonate minerals. *Anal.*
671 *Chem.*, 83(6), 2220-2226. <https://pubs.acs.org/doi/full/10.1021/ac103111y>.

672

673 Baer, D.S., Paul, J.B., Gupta, M. and O'Keefe, A., 2002. Sensitive absorption
674 measurements in the near-infrared region using off-axis integrated-cavity-output
675 spectroscopy. *Appl. Phys. B-Laser O.*, 75(2-3), 261-265.
676 <https://doi.org/10.1007/s00340-002-0971-z>.

677

678 Berden, G., Peeters, R. and Meijer, G., 2000. Cavity ring-down spectroscopy:
679 Experimental schemes and applications. *Int. Rev. Phys. Chem.*, vol. 19, 565-607.
680 <https://doi.org/10.1080/014423500750040627>.

681

682 Bowling, D.R., Baldocchi, D.D., Monson, R.K., 1999. Dynamics of isotopic exchange
683 of carbon dioxide in a Tennessee deciduous forest. *Global Biogeochem. Cycles* 13, 903-
684 922. <https://doi.org/10.1029/1999GB900072>.

685

686 Bowling, D.R., Sargent, S.D., Tanner, B.D., Ehleringer, J.R., 2003. Tunable diode laser
687 absorption spectroscopy for stable isotope studies of ecosystem-atmosphere CO_2
688 exchange. *Agr Forest Meteorol.* 118, 1-19. <https://doi.org/10.1016/S0168->
689 [1923\(03\)00074-1](https://doi.org/10.1016/S0168-1923(03)00074-1).

690 Brand, W.A., 2004. Mass spectrometer hardware for analyzing stable isotope ratios.
691 Handbook of stable isotope analytical techniques, 1, 835-856.
692 <https://doi.org/10.1016/B978-044451114-0/50040-5>.

693

694 Brenna, J.T., 1997. Use of stable isotopes to study fatty acid and lipoprotein metabolism
695 in man. Prostaglandins Leukot Essent Fatty Acids., 57(4), 467-472.
696 [https://doi.org/10.1016/S0952-3278\(97\)90430-0](https://doi.org/10.1016/S0952-3278(97)90430-0).

697

698 Brenna, J.T., Corso, T.N., Tobias, H.J. and Caimi, R.J., 1997. High-precision
699 continuous-flow isotope ratio mass spectrometry. Mass Spectrom. Rev., 16(5), 227-
700 258. [https://doi.org/10.1002/\(SICI\)1098-2787\(1997\)16:5<227::AID-MAS1>3.0.CO;2-J](https://doi.org/10.1002/(SICI)1098-2787(1997)16:5<227::AID-MAS1>3.0.CO;2-J).

701

702 Campbell Scientific, Inc. (TGA Series Trace Gas Analysers Revision: 10/18,
703 <https://s.campbellsci.com/documents/us/manuals/tga-series-trace-gas-analyzers.pdf>,
704 accessed 01 August 2019).

705

706 Carter, J.F., Barwick, V.J., 2011. Good Practice Guide for Isotope Ratio Mass
707 Spectrometry, FIRMS Network. p. 41.

708

709 Crosson, E. R., 2008. A cavity ring-down analyzer for measuring atmospheric levels of
710 methane, carbon dioxide, and water vapor. Applied Physics B., 92(3), 403-408.
711 <https://doi.org/10.1007/s00340-008-3135-y>.

712

713 Crosson, E.R., Ricci, K.N., Richman, B.A., Chilese, F.C., Owano, T.G., Provencal,
714 R.A., Todd, M.W., Glasser, J., Kachanov, A.A., Paldus, B.A., Spence, T.G., Zare, R.N.,
715 2002. Stable isotope ratios using cavity ring-down spectroscopy: determination of
716 $^{13}\text{C}/^{12}\text{C}$ for carbon dioxide in human breath,” Anal. Chem., 74, 2003-2007.
717 <https://doi.org/10.1021/ac025511d>.
718
719 Castrillo, A., Casa, G. and Gianfrani, L., 2007. Oxygen isotope ratio measurements in
720 CO_2 by means of a continuous-wave quantum cascade laser at 4.3 μm . Optics letters,
721 32(20), 3047-3049. <https://doi.org/10.1364/OL.32.003047>.
722
723 Dawson, T.E., and Simonin K.A., 2011. The roles of stable isotopes in forest hydrology
724 and biogeochemistry. Forest Hydrology and Biogeochemistry. Springer Netherlands,
725 137-161. https://doi.org/10.1007/978-94-007-1363-5_7.
726
727 Dickinson, D., Bodé, S. and Boeckx, P., 2017. Measuring ^{13}C -enriched CO_2 in air
728 with a cavity ring-down spectroscopy gas analyser: Evaluation and calibration. Rapid
729 Commun. Mass Spectrom., 31(22), 1892-1902. <https://doi.org/10.1002/rcm.7969>.
730
731 Dubbert, M., Cuntz, M., Piayda, A., Werner, C., 2014. Oxygen isotope signatures of
732 transpired water vapor: the role of isotopic non-steady-state transpiration under natural
733 conditions. New Phytol. 203, 1242-1252. <https://doi.org/10.1111/nph.12878>.
734
735 Edwards, G.C., Neumann, H.H., den Hartog, G., Thurtell, G.W., Kidd G., 1994. Eddy
736 correlation measurements of methane fluxes using a tunable diode laser at the Kinosheo

737 Lake tower site during the Northern Wetlands Study (NOWES), *J. Geophys. Res.*, 99,
738 1511-1517. <https://doi.org/10.1029/93JD02368>.

739

740 Elliott, B.M., Sung, K. and Miller, C.E., 2014. FT-IR spectra of ^{17}O -enriched CO_2 in
741 the ν_3 region: High accuracy frequency calibration and spectroscopic constants for
742 $^{16}\text{O}^{12}\text{C}^{17}\text{O}$, $^{17}\text{O}^{12}\text{C}^{17}\text{O}$, and $^{17}\text{O}^{12}\text{C}^{18}\text{O}$. *J. Mol. Spectrosc.*, 304, 1-11.
743 <https://doi.org/10.1016/j.jms.2014.08.001>.

744

745 Erdelyi, M., Richter, D., Tittel, F.K., 2002. $^{13}\text{CO}_2/^{12}\text{CO}_2$ isotopic ratio measurements
746 using a difference frequency-based sensor operating at 4.35 μm . *Appl. Phys. B: Lasers*
747 *and Optics.*, 75, 289-295. <https://doi.org/10.1007/s00340-002-0960-2>.

748

749 Esler, M.B., Griffith, D.W.T., Wilson, S.R. and Steele, L.P., 2000. Precision trace gas
750 analysis by FT-IR spectroscopy. 2. The $^{13}\text{C}/^{12}\text{C}$ isotope ratio of CO_2 . *Anal. Chem.*,
751 72(1), 216-221. <https://doi.org/10.1021/ac990563x>.

752

753 Faist, J., Capasso, F., Sivco, D.L., Sirtori, C., Hutchinson, A.L. and Cho, A.Y., 1994.
754 Quantum cascade laser. *Science-AAAS-Weekly Paper Edition-including Guide to*
755 *Scientific Information*, 264(5158), 553-555.
756 <https://doi.org/10.1126/science.264.5158.553>.

757

758 Ferretti, D.F., Lowe, D.C., Martin, R.J. and Brailsford, G.W., 2000. A new gas
759 chromatograph-isotope ratio mass spectrometry technique for high-precision, N_2O

760 free analysis of $\delta^{13}\text{C}$ and $\delta^{18}\text{O}$ in atmospheric CO_2 from small air samples. *J. Geophys.*
761 *Res. Atmos.*, 105(D5), 6709-6718. <https://doi.org/10.1029/1999JD901051>.
762
763 Flanagan, L.B. and Farquhar, G.D., 2014. Variation in the carbon and oxygen isotope
764 composition of plant biomass and its relationship to water-use efficiency at the leaf
765 and ecosystem scales in a northern Great Plains grassland. *Plant, cell & environment*,
766 37(2), 425-438. <https://doi.org/10.1111/pce.12165>.
767
768 Flores, E., Viallon, J., Moussay, P., Griffith, D.W.T. and Wielgosz, R.I., 2017.
769 Calibration Strategies for FT-IR and Other Isotope Ratio Infrared Spectrometer
770 Instruments for Accurate $\delta^{13}\text{C}$ and $\delta^{18}\text{O}$ Measurements of CO_2 in Air. *Anal. Chem.*,
771 89(6), 3648-3655. <https://doi.org/10.1021/acs.analchem.6b05063>.
772
773 Fry, B., 2006. *Stable Isotope Ecology*, Springer, New York, US. p. 308.
774 <https://doi.org/10.1007/0-387-33745-8>.
775
776 Glewen, W., 2007. Schematic illustration of Fourier-transform infrared spectroscopy.
777 (<https://www.slideserve.com/romney/fourier-transform-infrared-spectroscopy>, accessed
778 14 January 2019).
779
780 Griffis, T.J., Zhang, J., Baker, J.M., Kljun, N. and Billmark, K., 2007. Determining
781 carbon isotope signatures from micrometeorological measurements: Implications for
782 studying biosphere-atmosphere exchange processes. *Bound.-Layer Meteorol.*, 123(2),
783 295-316. <https://doi.org/10.1007/s10546-006-9143-8>.

784

785 Griffis, T.J., Sargent, S.D., Baker, J.M., Lee, X., Tanner, B.D., Greene, J., Swiatek, E.
786 and Billmark, K., 2008. Direct measurement of biosphere-atmosphere isotopic CO₂
787 exchange using the eddy covariance technique. *J. Geophys. Res.*, 113(D8).
788 <https://doi.org/10.1029/2007JD009297>.

789

790 Griffis, T.J., Sargent, S.D., Lee, X., Baker, J.M., Greene, J., Erickson, M., Zhang, X.,
791 Billmark, K., Schultz, N., Xiao, W., Hu, N., 2010. Determining the oxygen isotope
792 composition of evapotranspiration using eddy covariance. *Bound. Layer Meteorol.* 137
793 (2), 307-326. <https://doi.org/10.1007/s10546-010-9529-5>.

794

795 Griffis, T.J., 2013. Tracing the flow of carbon dioxide and water vapor between the
796 biosphere and atmosphere: A review of optical isotope techniques and their application.
797 *Agric. For. Meteorol.*, 174, 85-109. <https://doi.org/10.1016/j.agrformet.2013.02.009>.

798

799 Griffith, D.W.T., Deutscher, N., Caldw, C., Kettlewell, G., Riggensbach, M., Hammer,
800 S., 2012. A fourier transform infrared trace gas analyzer for atmospheric applications.
801 *Atmos. Measur. Tech.*, 5, 2481-2498. <https://doi.org/10.5194/amtd-5-3717-2012>.

802

803 Griffith, D.W.T., 2018. Calibration of isotopologue-specific optical trace gas analysers:
804 a practical guide. *Atmos. Meas. Tech.*, 11, 6189–6201. [http://dx.doi.org/10.5194/amt-](http://dx.doi.org/10.5194/amt-11-6189-2018)
805 [11-6189-2018](http://dx.doi.org/10.5194/amt-11-6189-2018).

806

807 Gordon, I.E., Rothman, L.S., Hill, C., Kochanov, R.V., Tan, Y., Bernath, P.F., Birk, M.,
808 Boudon, V., Campargue, A., Chance, K.V. and Drouin, B.J., 2017. The HITRAN2016
809 molecular spectroscopic database. *J. Quant. Spectrosc. Ra.*, 203, pp.3-69.
810 <https://doi.org/10.1016/j.jqsrt.2017.06.038>.

811 Guillon, S., Pili, E., Agrinier, P. 2012. Using a laser-based CO₂ carbon isotope analyser
812 to investigate gas transfer in geological media. *Appl. Phys. B. Lasers Opt.* 107, 449-
813 457. <https://doi.org/10.1007/s00340-012-4942-8>.

814

815 Gupta, M., 2012. Cavity-enhanced laser absorption spectrometry for industrial
816 applications. *Gases Instrum.*, 6, 23-28. [http://67.20.113.103/resources/appnotes/Cavity-
817 Enhanced%20Laser%20Absorption%20Spectrometry%20for%20Industrial%20Applica
818 tions%20May_June%202012.pdf](http://67.20.113.103/resources/appnotes/Cavity-Enhanced%20Laser%20Absorption%20Spectrometry%20for%20Industrial%20Applications%20May_June%202012.pdf) (accessed 14 January 2019).

819

820 Hammer, S., Griffith, D.W.T., Konrad, G., Vardag, S., Caldow, C. and Levin, I., 2012.
821 Assessment of a multi-species in-situ FTIR for precise atmospheric greenhouse gas
822 observations. *Atmos. Meas. Tech. Disc.*, 5, 3645-3692. [https://doi.org/10.5194/amt-6-
823 1153-2013](https://doi.org/10.5194/amt-6-1153-2013).

824

825 Hovorka, J., Čermák, P. and Veis, P., 2017. Optimization of data retrieval process for
826 spectroscopic CO₂ isotopologue ratio measurements. *Laser Phys.*, 27(5), p.055701.
827 <https://doi.org/10.1088/1555-6611/aa64b8>.

828

829 Hendry, M.J., Schmeling, E., Wassenaar, L.I., Barbour, S.L. and Pratt, D., 2015.
830 Determining the stable isotope composition of pore water from saturated and

831 unsaturated zone core: improvements to the direct vapour equilibration laser
832 spectrometry method. *Hydrol. Earth Syst. Sci.*, 19(11), p. 4427.
833 <https://doi.org/10.5194/hess-19-4427-2015>.

834

835 Hill, C., Gordon, I.E., Kochanov, R.V., Barrett, L., Wilzewski, J.S. and Rothman, L.S.,
836 2016. HITRANonline: An online interface and the flexible representation of
837 spectroscopic data in the HITRAN database. *J. Quant. Spectrosc. Ra.*, 177, 4-14.
838 <https://doi.org/10.1016/j.jqsrt.2015.12.012>

839

840 Hoefs, J. 2009. Theoretical and experimental principles. *Stable Isotope Geochemistry*,
841 1-46. https://doi.org/10.1007/978-3-319-19716-6_1.

842

843 Huang, X., Schwenke, D.W., Freedman, R.S. and Lee, T.J., 2017. Ames-2016 line lists
844 for 13 isotopologues of CO₂: Updates, consistency, and remaining issues. *J. Quant.*
845 *Spectrosc. Ra.*, 203, 224-241. <https://doi.org/10.1016/j.jqsrt.2017.04.026>.

846

847 Jacquinet-Husson, N., Armante, R., Scott, N.A., Chédin, A., Crépeau, L., Boutamine,
848 C., Bouhdaoui, A., Crevoisier, C., Capelle, V., Boone, C. and Poulet-Crovisier, N.,
849 2016. The 2015 edition of the GEISA spectroscopic database. *J. Mol. Spectrosc.*, 327,
850 31-72. <https://doi.org/10.1016/j.jms.2016.06.007>.

851

852 Jochheim, H., Wirth, S. and von Unold, G., 2017. A multi-layer, closed-loop system
853 for continuous measurement of soil CO₂ concentration. *J. Plant Nutr. Soil Sci.* 1-8.
854 <https://doi.org/10.1002/jpln.201700259>.

855

856 Joos, O., Saurer, M., Heim, A., Hagedorn, F., Schmidt, M.W. and Siegwolf, R.T., 2008.
857 Can we use the CO₂ concentrations determined by continuous-flow isotope ratio mass
858 spectrometry from small samples for the Keeling plot approach? *Rapid Commun. Mass*
859 *Spectrom.*, 22(24), 4029-4034. <https://doi.org/10.1002/rcm.3827>.

860

861 Karlovets, E.V., Sidorenko, A.D., Čermák, P., Mondelain, D., Kassi, S., Perevalov, V.I.
862 and Campargue, A., 2018. The ¹³CO₂ absorption spectrum by CRDS near 1.74 μm. *J.*
863 *Mol. Spectrosc.*, 354, 54-59. <https://doi.org/10.1016/j.jms.2018.10.003>.

864

865 Keeling, C.D., 1958. The concentration and isotopic abundances of atmospheric carbon
866 dioxide in rural areas. *Geochim. Cosmochim. Acta.*, 13(4), 322-334.
867 [https://doi.org/10.1016/0016-7037\(58\)90033-4](https://doi.org/10.1016/0016-7037(58)90033-4).

868

869 Kerstel, E. and Gianfrani, L., 2008. Advances in laser-based isotope ratio
870 measurements: selected applications. *Appl. Phys. B: Lasers Opt.*, 92(3), 439-449.
871 <https://doi.org/10.1007/s00340-008-3128-x>.

872

873 Kerstel, E.R.Th., van Trigt, R., Dam, N., Reuss, J., Meijer, H.A.J., 1999. Simultaneous
874 determination of the 2H/1H, ¹⁷O/¹⁶O, and ¹⁸O/¹⁶O isotope abundance ratios in water by
875 means of laser spectrometry. *Anal. Chem.*, 71, 5297-5303.
876 <https://doi.org/10.1021/ac990621e>.

877

878 Linnerud, I., Kaspersen, P. and Jaeger, T., 1998. Gas monitoring in the process industry
879 using diode laser spectroscopy. *Appl Phys B-Lasers O.*, 67(3), 297-305.
880 <https://doi.org/10.1007/s003400050509>.

881

882 ABB - Los Gatos Research (<http://www.lgrinc.com/analyzers/isotope/>, accessed 01
883 August 2019).

884

885 Mahesh, P., Sreenivas, G., Rao, P.V.N., Dadhwal, V.K., Sai Krishna, S.V.S.,
886 Mallikarjun, K., 2015. High-precision surface-level CO₂ and CH₄ using offaxis
887 integrated cavity output spectroscopy (OA-ICOS) over Shadnagar, India. *Int. J. Remote*
888 *Sens.* vol. 36, no. 22, 5754-5765. <https://doi.org/10.1080/01431161.2015.1104744>.

889

890 Maher, D.T., Santos, I.R. and Tait, D.R., 2014. Mapping Methane and Carbon Dioxide
891 Concentrations and $\delta^{13}\text{C}$ Values in the Atmosphere of Two Australian Coal Seam Gas
892 Fields. *Water Air Soil Pollut.*, 225:2216. <http://dx.doi.org/10.1007/s11270-014-2216-2>.

893

894 Marron, N., Plain, C., Longdoz, B., Epron, D., 2009. Seasonal and daily time course of
895 the ^{13}C composition in soil CO₂ efflux recorded with a tunable diode laser
896 spectrophotometer (TDLS), *Plant Soil.*, 318, 137-151. [https://doi.org/10.1007/s11104-](https://doi.org/10.1007/s11104-008-9824-9)
897 [008-9824-9](https://doi.org/10.1007/s11104-008-9824-9).

898

899 McAlexander, I., Rau, G.H., Liem, J., Owano, T., Fellers, R., Baer, D., Gupta, M.,
900 2011. Deployment of a Carbon Isotope Ratiometer for the Monitoring of CO₂

901 Sequestration Leakage. Anal. Chem., 83(16), 6223-6229.
902 <https://doi.org/10.1021/ac2007834>.

903

904 McDonagh, C., Burke, C. S., MacCraith, B. D., 2008. Optical Chemical Sensors. Chem.
905 Rev., 108, 400-422. <https://doi.org/10.1021/cr068102g>.

906

907 McDowell, N., Pockman, W. T., Allen, C. D., Breshears, D. D., Cobb, N., Kolb, T., ...
908 & Yezzer, E. A., 2008. Mechanisms of plant survival and mortality during drought: why
909 do some plants survive while others succumb to drought? New phytologist, 178(4), 719-
910 739. <https://doi.org/10.1111/j.1469-8137.2008.02436.x>.

911

912 Michener, R., and Lajtha, K., 2008. In: Michener R.H., Lajtha K. (Eds.), Stable Isotopes
913 in Ecology and Environmental Science (2nd ed.), John Wiley & Sons, p. 592.
914 <https://doi.org/10.1002/9780470691854>.

915

916 Midwood, A.J. and Millard, P., 2011. Challenges in measuring the $\delta^{13}\text{C}$ of the soil
917 surface CO_2 efflux. Rapid Commun. Mass Spectrom., 25(1), 232-242.
918 <https://doi.org/10.1002/rcm.4857>.

919

920 Mortazavi, B. and Chanton, J.P., 2002. A rapid and precise technique for measuring
921 $\delta^{13}\text{C}$ in CO_2 and $\delta^{18}\text{O}$ in CO_2 ratios at ambient CO_2 concentrations for biological
922 applications and the influence of container type and storage time on the sample isotope
923 ratios. Rapid Commun. Mass Spectrom., 16(14), 1398-1403.
924 <https://doi.org/10.1002/rcm.730>.

925

926 Morville, J., Kassi, S., Chenevier, M., Romanini, D., 2005. Fast, low-noise, mode-by-
927 mode, cavity-enhanced absorption spectroscopy by diode-laser self-locking. Appl. Phys.
928 B: Lasers Opt., 80, 1027-1038. <https://doi.org/10.1007/s00340-005-1828-z>.

929

930 Muccio, Z. and Jackson, G.P., 2009. Isotope ratio mass spectrometry. Analyst, 134(2),
931 213-222. <https://doi.org/10.1039/B808232D>.

932 Munksgaard, N.C., Davies, K., Wurster, C.M., Bass, A.M. and Bird, M.I., 2013. Field-
933 based cavity ring-down spectrometry of $\delta^{13}\text{C}$ in soil-respired CO_2 . Isotopes Environ
934 Health Stud., 49(2), 232-242. <https://doi.org/10.1080/10256016.2013.750606>.

935

936 Nelson, D.D., McManus, J.B., Herndon, S.C., Zahniser, M.S., Tuzson, B. and
937 Emmenegger, L., 2008. New method for isotopic ratio measurements of atmospheric
938 carbon dioxide using a 4.3 μm pulsed quantum cascade laser. Appl. Phys. B: Lasers and
939 Optics, 90(2), 301-309. <https://doi.org/10.1007/s00340-007-2894-1>.

940

941 Nier, A.O., 1940. A mass spectrometer for routine isotope abundance measurements.
942 Rev. Sci. Instrum., 11(7), 212-216. <https://doi.org/10.1063/1.1751688>.

943

944 Nowakowski, M., Wojtas, J., Bielecki, Z. and Mikołajczyk, J., 2009. Cavity enhanced
945 absorption spectroscopy sensor. Acta Physica Polonica-Series A General Physics,
946 116(3), 363. <https://doi.org/10.12693/APhysPolA.116.363>.

947

948 Ogée, J., Peylin, P., Ciais, P., Bariac, T., Brunet, Y., Berbigier, P., Roche, C., Richard,
949 P., Bardoux, G., Bonnefond, J.-M., 2003. Partitioning net ecosystem carbon exchange
950 into net assimilation and respiration using $^{13}\text{CO}_2$ measurements: A cost-effective
951 sampling strategy. *Global Biogeochem. Cycles* 17 (2).
952 <https://doi.org/10.1029/2002GB001995>.
953
954 O'Keefe, A., Deacon, D.A.G., 1988 Cavity ring-down optical spectrometer for
955 absorption measurements using pulsed laser sources. *Rev. Sci. Instrum.* 59, 2544-51.
956 <https://doi.org/10.1063/1.1139895>.
957 Orłowski, N., Pratt, D. L., & McDonnell, J. J., 2016. Intercomparison of soil pore water
958 extraction methods for stable isotope analysis. *Hydrol. Process.* 30(19), 3434-3449.
959 <https://doi.org/10.1002/hyp.10870>.
960
961 Pachauri, R.K., Allen, M.R., Barros, V.R., Broome, J., Cramer, W., Christ, R., Church,
962 J.A., Clarke, L., Dahe, Q., Dasgupta, P. and Dubash, N.K., 2014. Climate change 2014:
963 Synthesis Report. Contribution of working groups I, II and III to the fifth assessment
964 report of the intergovernmental panel on climate change. IPCC, p.151.
965 <https://doi.org/10013/epic.45156.d001>.
966
967 Paldus, B.A., Harb, C.C., Spence, T.G., Wilke, B., Xie, J., Harris, J.S., Zare, R.N.,
968 1998. Cavity-locked ring-down spectroscopy. *J. Appl. Phys.*, 83, 3991-3997.
969 <https://doi.org/10.1063/1.367155>.
970

971 Paul, J. B., Lapson, L. and Anderson, J. G., 2001. Ultrasensitive absorption
972 spectroscopy with a high-finesse optical cavity and off-axis alignment. Appl. Opt.,
973 40(27), 4904-4910. <https://doi.org/10.1364/AO.40.004904>.
974

975 Picarro, Inc. (http://www.picarro.com/technology/cavity_ring_down_spectroscopy,
976 accessed 01 August 2019).
977

978 Pogány, A., Ott, O., Werhahn, O. and Ebert, V., 2013. Towards traceability in CO₂ line
979 strength measurements by TDLAS at 2.7 μm. J. Quant. Spectrosc.Ra., 130, 147-157.
980 <https://doi.org/10.1016/j.jqsrt.2013.07.011>.
981

982 Rao, M. S., 2012. Stable Isotopic Analysis Using Mass Spectrometry and Laser Based
983 Techniques: A Review. Int. J. Emerg. Trends Sci. Technol., Springer India, 523-538.
984 https://doi.org/10.1007/978-81-322-1007-8_48.
985

986 Ribas-Carbo, M., Still, C., Berry, J., 2002. Automated system for simultaneous
987 analysis of δ¹³C, δ¹⁸O and CO₂ concentrations in small air samples. Rapid Commun.
988 Mass Spectrom., 16(5), 339-345. <https://doi.org/10.1002/rcm.582>.
989

990 Riederer, M., Pausch, J., Kuzyakov, Y. and Foken, T., 2015. Partitioning NEE for
991 absolute C input into various ecosystem pools by combining results from eddy-
992 covariance, atmospheric flux partitioning and ¹³C CO₂ pulse labeling. Plant and Soil,
993 390(1-2), 61-76. <https://doi.org/10.1007/s11104-014-2371-7>.

994 Rothman, L.S., Gordon, I.E., Babikov, Y., Barbe, A., Benner, D.C., Bernath, P.F., Birk,
995 M., Bizzocchi, L., Boudon, V., Brown, L.R. and Campargue, A., 2013. The
996 HITRAN2012 molecular spectroscopic database. *J. Quant. Spectrosc. Ra.*, 130, 4-50.
997 <https://doi.org/10.1016/j.jqsrt.2013.07.002>.
998
999 Saleska, S.R., Shorter, J.H., Herndon, S., Jiménez, R., Barry McManus, J., William
1000 Munger, J., Nelson, D.D. and Zahniser, M.S., 2006. What are the instrumentation
1001 requirements for measuring the isotopic composition of net ecosystem exchange of CO₂
1002 using eddy covariance methods? *Isot. Environ. Health Stud.*, 42(2), 115-133.
1003 <https://doi.org/10.1080/10256010600672959>.
1004
1005 Santos, E., Wagner-Riddle, C., Lee, X., Warland, J., Brown, S., Staebler, R., Bartlett, P.
1006 and Kim, K., 2012. Use of the isotope flux ratio approach to investigate the C¹⁸O¹⁶O
1007 and ¹³CO₂ exchange near the floor of a temperate deciduous forest. *Biogeosciences*,
1008 9(7), 2385-2399. <https://doi.org/10.5194/bg-9-2385-2012>.
1009
1010 Schaeffer, S.M., Miller, J.B., Vaughn, B.H., White, J.W.C., Bowling, D.R., 2008. Long-
1011 term field performance of a tunable diode laser absorption spectrometer for analysis of
1012 carbon isotopes of CO₂ in forest air. *Atmos. Chem. Phys.*, 8, 5263-5277.
1013 <https://doi.org/10.5194/acp-8-5263-2008>.
1014
1015 Schauer, A.J., Lott, M.J., Cook, C.S., & Ehleringer, J.R., 2005. An automated system
1016 for stable isotope and concentration analyses of CO₂ from small atmospheric samples.
1017 *Rapid Commun. Mass Spectrom.*, 19(3), 359-362. <https://doi.org/10.1002/rcm.1792>.

1018

1019 Schimel, D., Pavlick, R., Fisher, J. B., Asner, G. P., Saatchi, S., Townsend, P., ... &
1020 Cox, P., 2015. Observing terrestrial ecosystems and the carbon cycle from space. *Global*
1021 *change biol.*, 21(5), 1762-1776. <https://doi.org/10.1111/gcb.12822>.

1022

1023 Schnyder, H., Schäufele, R., Wenzel, R., 2004. Mobile, outdoor continuous-flow
1024 isotope-ratio mass spectrometer system for automated high-frequency ^{13}C -and ^{18}O - CO_2
1025 analysis for Keeling plot applications. *Rapid Commun. Mass Spectrom.*, 18(24), 3068-
1026 3074. <https://doi.org/10.1002/rcm.1731>.

1027

1028 Shuk, P., and Jantz, R., 2015. Oxygen gas sensing technologies: A comprehensive
1029 review. In 2015 9th International Conference on Sensing Technology (ICST), 12-17.
1030 IEEE. <https://doi.org/10.1109/ICSensT.2015.7438356>.

1031

1032 Sigrist, M. W., Bartlome, R., Marinov, D., Rey, J. M., Vogler, D. E., Wächter, H., 2008.
1033 Trace gas monitoring with infrared laser-based detection schemes. *Appl. Phys. B* 90,
1034 289-300. <https://doi.org/10.1007/s00340-007-2875-4>.

1035

1036 Sprenger, M., Tetzlaff, D. and Soulsby, C., 2017. No influence of CO_2 on stable isotope
1037 analyses of soil waters with off-axis integrated cavity output spectroscopy (OA-
1038 ICOS). *Rapid Commun. Mass Spectrom.*, 31(5), 430-436.
1039 <https://doi.org/10.1002/rcm.7815>.

1040

1041 Sulzman, E.W., 2007. Stable Isotopes in Ecology and Environmental Science, Chapter
1042 1, In: Michener R.H. and Lajtha K. (Eds.), Stable Isotopes in Ecology and
1043 Environmental Science, 2nd edition, Blackwell Publishing, 1-23.
1044 <https://doi.org/10.1002/9780470691854>.

1045

1046 Stropes, K.S., 2017. Investigating the exchange of CO₂ in a tall-grass prairie ecosystem
1047 using stable isotopes and micrometeorological methods (Doctoral dissertation, Kansas
1048 State University), p. 107. <http://hdl.handle.net/2097/34634>.

1049

1050 Sturm, P., Eugster, W. and Knohl, A., 2012. Eddy covariance measurements of CO₂
1051 isotopologues with a quantum cascade laser absorption spectrometer. Agric. For.
1052 Meteorol., 152, 73-82. <https://doi.org/10.1016/j.agrformet.2011.09.007>.

1053 Tans, P.P., Crotwell, A.M. and Thoning, K.W., 2017. Abundances of isotopologues and
1054 calibration of CO₂ greenhouse gas measurements. Atmos. Meas. Tech., 10(7), 2669-
1055 2685. <https://doi.org/10.5194/amt-10-2669-2017>.

1056

1057 Tashkun, S.A., Perevalov, V.I., Gamache, R.R. and Lamouroux, J., 2015. CDS-296,
1058 high resolution carbon dioxide spectroscopic databank: Version for atmospheric
1059 applications. J. Quant. Spectrosc. Ra., 152, 45-73.
1060 <https://doi.org/10.1016/j.jqsrt.2014.10.017>.

1061

1062 Tashkun, S.A., Perevalov, V.I., Gamache, R.R. and Lamouroux, J., 2019. CDS-296,
1063 high-resolution carbon dioxide spectroscopic databank: An update. J. Quant. Spectrosc.
1064 Ra., 228, 124-131. <https://doi.org/10.1016/j.jqsrt.2019.03.001>.

1065

1066 Theis, D.E., Saurer, M., Blum, H., Frossard, E. and Siegwolf, R.T., 2004. A portable
1067 automated system for trace gas sampling in the field and stable isotope analysis in the
1068 laboratory. *Rapid Commun. Mass Spectrom.*, 18(18), 2106-2112.
1069 <https://doi.org/10.1002/rcm.1596>.

1070

1071 Tittel, F.K., Lewicki, R., Lascola, R. and McWhorter, S., 2013. Emerging infrared laser
1072 absorption spectroscopic techniques for gas analysis. *Trace Analysis of Specialty and*
1073 *Electronic Gases*, edited by: Geiger, WM and Raynor, MW, 71-109.
1074 <https://doi.org/10.1002/9781118642771.ch4>.

1075

1076 Tohjima, Y., Katsumata, K., Morino, I., Mukai, H., Machida, T., Akama, I., Amari, T.
1077 and Tsunogai, U., 2009. Theoretical and experimental evaluation of the isotope effect of
1078 NDIR analyzer on atmospheric CO₂ measurement. *J. Geophys. Res-Atmos.*, 114.
1079 <https://doi.org/10.1029/2009JD011734>.

1080

1081 Toth, R.A., Brown, L.R., Miller, C.E., Devi, V.M. and Benner, D.C., 2008.
1082 Spectroscopic database of CO₂ line parameters: 4300–7000 cm⁻¹. *J. Quant. Spectrosc.*
1083 *Ra.*, 109(6), 906-921. <https://doi.org/10.1016/j.jqsrt.2007.12.004>.

1084

1085 Tuzson, B., Mohn, J., Zeeman, M.J., Werner, R.A., Eugster, W., Zahniser, M.S.,
1086 Nelson, D.D., McManus, J.B. and Emmenegger, L., 2008. High precision and
1087 continuous field measurements of $\delta^{13}\text{C}$ and $\delta^{18}\text{O}$ in carbon dioxide with a cryogen-

1088 free QCLAS. Appl. Phys. B: Lasers and Optics, 92(3), 451-458.
1089 <https://doi.org/10.1007/s00340-008-3085-4>.
1090
1091 Tuzson, B., Henne, S., Brunner, D., Steinbacher, M., Mohn, J., Buchmann, B. and
1092 Emmenegger, L., Continuous isotopic composition measurements of tropospheric CO₂
1093 at Jungfraujoch (3580 m asl), Switzerland: real-time observation of regional pollution
1094 events. Atmos. Chem. Phys. 11 (4), 2011, 1685-1696, [https://doi.org/10.5194/acp-11-](https://doi.org/10.5194/acp-11-1685-2011)
1095 [1685-2011](https://doi.org/10.5194/acp-11-1685-2011).
1096
1097 van Geldern, R., Nowak, M. E., Zimmer, M., Szizybalski, A., Myrntinen, A., Barth, J.
1098 A., & Jost, H. J., 2014. Field-based stable isotope analysis of carbon dioxide by mid-
1099 infrared laser spectroscopy for carbon capture and storage monitoring. Anal Chem.,
1100 86(24), 12191-12198. <https://doi.org/10.1021/ac5031732>.
1101
1102 Vaughn, B.H., Evans, C.U., White, J.W., Still, C.J., Masarie, K.A. and Turnbull, J.,
1103 2010. Global network measurements of atmospheric trace gas isotopes. In Isoscapes.
1104 Springer Netherlands, 3-31. https://doi.org/10.1007/978-90-481-3354-3_1.
1105
1106 Von Sperber, C., Weiler, M. and Brüggemann, N., 2015. The effect of soil moisture,
1107 soil particle size, litter layer and carbonic anhydrase on the oxygen isotopic composition
1108 of soil-released CO₂. Eur. J. Soil Sci. 66(3), 566-576.
1109 <https://doi.org/10.1111/ejss.12241>.
1110

1111 Wada, R., Matsumi, Y., Takanashi, S., Nakai, Y., Nakayama, T., Ouchi, M., Hiyama,
1112 T., Fujiyoshi, Y., Nakano, T., Kurita, N. and Muramoto, K., 2016. In situ measurement
1113 of CO₂ and water vapour isotopic compositions at a forest site using mid-infrared laser
1114 absorption spectroscopy. *Isotopes Environ. Health Stud.*, 52(6), 603-618.
1115 <https://doi.org/10.1080/10256016.2016.1147441>.

1116

1117 Wada, R., Matsumi, Y., Nakayama, T., Hiyama, T., Fujiyoshi, Y., Kurita, N.,
1118 Muramoto, K., Takanashi, S., Kodama, N. and Takahashi, Y., 2017. Continuous
1119 measurements of stable isotopes of carbon dioxide and water vapour in an urban
1120 atmosphere: isotopic variations associated with meteorological conditions. *Isotopes
1121 Environ. Health Stud.*, 53(6), 646-659. <https://doi.org/10.1080/10256016.2017.1348351>.

1122

1123 Waechter, H., Litman, J., Cheung, A.H., Barnes, J.A. and Loock, H.P., 2010. Chemical
1124 sensing using fiber cavity ring-down spectroscopy. *Sensors*, 10(3), 716-1742.
1125 <https://doi.org/10.3390/s100301716>.

1126

1127 Wehr, R., Munger, J.W., Nelson, D.D., McManus, J.B., Zahniser, M.S., Wofsy, S.C.
1128 and Saleska, S.R., 2013. Long-term eddy covariance measurements of the isotopic
1129 composition of the ecosystem–atmosphere exchange of CO₂ in a temperate
1130 forest. *Agric. For. Meteorol.*, 181, 69-84.
1131 <https://doi.org/10.1016/j.agrformet.2013.07.002>.

1132

1133 Wehr, R., and Saleska, S.R., 2015. An improved isotopic method for partitioning net
1134 ecosystem–atmosphere CO₂ exchange. *Agric. For. Meteorol.*, 214, 515-531.
1135 <https://doi.org/10.1016/j.agrformet.2015.09.009>.
1136

1137 Wehr, R., Munger, J. W., McManus, J. B., Nelson, D. D., Zahniser, M. S., Davidson, E.
1138 A., and Saleska, S. R., 2016. Seasonality of temperate forest photosynthesis and
1139 daytime respiration. *Nature*, 534 (7609), 680. <https://doi.org/10.1038/nature17966>.
1140

1141 Wehr, R., Commane, R., Munger, J. W., McManus, J. B., Nelson, D. D., Zahniser, M.
1142 S., and Wofsy, S. C., 2017. Dynamics of canopy stomatal conductance, transpiration,
1143 and evaporation in a temperate deciduous forest, validated by carbonyl sulfide uptake.
1144 *Biogeosciences*, 14(2), 389-401. <https://doi.org/10.5194/bg-14-389-2017>.
1145

1146 Wen, X. F., Lee, X., Sun, X. M., Wang, J. L., Tang, Y. K., Li, S. G., & Yu, G. R., 2012.
1147 Intercomparison of four commercial analyzers for water vapor isotope measurement. *J.*
1148 *Atmos. Oceanic Technol.*, 29(2), 235-247.
1149

1150 Wen, X.F., Meng, Y., Zhang, X.Y., Sun, X.M. and Lee, X., 2013. Evaluating calibration
1151 strategies for isotope ratio infrared spectroscopy for atmospheric ¹³CO₂/¹²CO₂
1152 measurement. *Atmospheric Meas. Tech.*, 6(6), 1491-150.
1153 <https://doi.org/10.1175/JTECH-D-10-05037.1>.
1154

1155 Wen, X., Yang, B., Sun, X. and Lee, X., 2016. Evapotranspiration partitioning through
1156 in-situ oxygen isotope measurements in an oasis cropland. *Agric. For. Meteorol.*, 230,
1157 89-96. <https://doi.org/10.1016/j.agrformet.2015.12.003>.
1158

1159 Werle, P., 1998. A review of recent advances in semiconductor laser based gas
1160 monitors. *Spectrochim. Acta A. Mol. Biomol. Spectrosc.*, 54(2), 197-236.
1161 [https://doi.org/10.1016/S1386-1425\(97\)00227-8](https://doi.org/10.1016/S1386-1425(97)00227-8).
1162

1163 Werle, P.W., Mazzinghi, P., D'Amato, F., De Rosa, M., Maurer, K. and Slemr, F.,
1164 2004. Signal processing and calibration procedures for in situ diode-laser absorption
1165 spectroscopy. *Spectrochim. Acta A. Mol. Biomol. Spectrosc.*, 60(8), 1685-1705.
1166 <https://doi.org/10.1016/j.saa.2003.10.013>.
1167

1168 West, A.G., Goldsmith, G. R., Matimati, I., Dawson, T. E., 2011. Spectral analysis
1169 software improves confidence in plant and soil water stable isotope analyses performed
1170 by isotope ratio infrared spectroscopy (IRIS). *Rapid Commun Mass Sp.*, 25(16), 2268-
1171 2274. <https://doi.org/10.1002/rcm.5126>.
1172

1173 Wingate, L., Ogée, J., Burette, R., Bosc, A., Devaux, M., Grace, J., Loustau, D. and
1174 Gessler, A., 2010. Photosynthetic carbon isotope discrimination and its relationship to
1175 the carbon isotope signals of stem, soil and ecosystem respiration. *New Phytologist*,
1176 188(2), 576-589. <https://doi.org/10.1111/j.1469-8137.2010.03384.x>.
1177

1178 Xia, L., Zhou, L., van der Schoot, M. V., Rella, C. W., Liu, L., Zhang, G., & Wang, H.,
1179 2016. Evaluation of the carbon isotopic effects of NDIR and CRDS analyzers on
1180 atmospheric CO₂ measurements. *Sci. China Earth*, 59(6), 1299-1307.
1181 <https://doi.org/10.1007/s11430-016-5294-8>.
1182
1183 Zeeman, M.J., Werner, R.A., Eugster, W., Siegwolf, R.T., Wehrle, G., Mohn, J.,
1184 Buchmann, N., 2008. Optimization of automated gas sample collection and isotope ratio
1185 mass spectrometric analysis of $\delta^{13}\text{C}$ of CO₂ in air. *Rapid Commun. Mass Spectrom.*,
1186 22(23), 3883-3892. <https://doi.org/10.1002/rcm.3772>.
1187
1188 Žak, E.J., 2017. Theoretical rotational-vibrational and rotational-vibrational-electronic
1189 spectroscopy of triatomic molecules (Doctoral dissertation, UCL (University College
1190 London)), p. 291. <http://discovery.ucl.ac.uk/id/eprint/10026185>.